UNIVERSITY OF TROMSØ UIT

FACULTY OF HEALTH SCIENCES

DEPARTMENT OF CLINICAL MEDICINE

UNIVERSITY HOSPITAL OF NORTH NORWAY

PEDIATRIC DEPARTMENT

mir-34a targets cell cycle genes *CCND1* (cyclin D1) and *MYCN*, while *mir-21* does not target *PTEN* and *PDCD4* in neuroblastoma

Peter Utnes

A Master Thesis in Molecular Biotechnology (MBI-3941)

June 2013

TABLE OF CONTENTS

Acknowledgements

This work was conducted at the Pediatric Research Group, University of Tromsø under the supervision of researcher Dr. Christer Einvik and PhD-student Bjørn-Helge Haug.

While conducting this work, I often resolved for help. Numerous members of our group could lend me a hand in times of need. I would especially like to thank my supervisor Christer Einvik for his in-depth expertise on research in general and on the complicated field of neuroblastoma. You have always been there when needed and have guided me in the right direction. Also, my co-supervisor Bjørn-Helge Haug, which have a profound knowledge on work in the laboratory as well as insight into the realms of the pediatric cancer that we all are working with, have been to tremendous help and have given me many brilliant ideas on how to solve my work.

To the boss, Prof. Trond Flægstad: Thank you for organizing, achieving funds, giving advice, and working in the background.

To our chief engineer, Cecilie Løkke: your kindness and help in the laboratory have always been to great help. Your experience is much appreciated!

To all my other companions in the laboratory (Simon Kranz, PhD-student Sarah Roth, Research student Øyvind Hald, PhD-student Swapnil Parashram Bhavsar), I would like to thank you for your support and for all our small-talks. Our working environment would not have been the same without you! I would also like to thank post docs Jørn Remi Henriksen and Jochen Büchner, which have been a part of the neuroblastoma research group and whose interest have presented the neuroblastoma community with valuable data.

I would like to thank everyone that has given me lectures that I have enjoyed during my path to a degree in molecular biotechnology: Associate Prof. Dag-Hugo Coucheron, Prof. Steinar Johansen, Prof. Terje Johansen, Prof. Raafat El-Gewely, Prof. Ugo Moens, Prof. Baldur Sveinbjørnsson, Researcher Dr. Morten Andreassen, Senior lecturer Dr. Gaute Hansen, Dr. Wim Dictus (UMC Utrecht), Dr. Joost Koedam (UMC Utrecht), Assistant Prof.

Geert M.J. Ramakers (UMC Utrecht), Kristin Denzer (UMC Utrecht), Dr. Adri Thomas (UMC Utrecht) and many more.

To my class and fellow students, our experience and discussions have been an enlightment during our five years together.

To everyone at the MH-building, for lending me a helping hand, borrowing reagents and for your expertise. A special thanks to our neighboring lab (Trine Tessem and co.) for using your PCR facilities and the RNA group (Prof. Steinar Johansen and Anita Ursvik) for borrowing reagents. Teamwork is the factor to success. Never hesitate to ask me for advice or other questions in the future. I would be happy to help.

To my family, for being there throughout my life, for safeguarding me, raising me, keeping me with companionship, for encouragement, for everything – you are always there for me when I need you. You have taught me how to be a future-coming, astonishing scientist!

My friends, for whom there are many, I would like to thank you very much for the times that you have spent with me. Being able to focus on other things than my work 24/7 has been much appreciated!

A special thanks to my dearest of all, Elise and Amanda, for your love and support. You are the ones that have given me the strength and energy to finish this thesis.

As this work has an aim to be presented in a scientific article, the group and the author claims that the reviewer of this thesis needs to maintain complete confidentiality.

1 Abbreviations

ago	argonaute
ALK	anaplastic lymphoma kinase
amp	ampicillin
AP-1	activator protein-1
AREs	AU-rich elements
ATP	adenosine triphosphate
bHLH	basic helix-loop-helix
bHLHLZ	bHLH leucine zipper
bi	biotin
bi-*mir-21*	biotin 3'-end-labeled *mir-21*
bi-*mir-34a*	biotin 3'-end-labeled *mir-34a*
BMP	bone morphogenetic protein
bp	base pair
cel	*Caenorhabditis elegans*
C/EBP-α	CCAAT-enhancer-binding protein-α
CCR4/NOT	C-C chemokine receptor 4-NOT
CDS	coding DNA sequence
CDK	cyclin dependent kinase
CDK4	cyclin dependent kinase 4
CDK6	cyclin dependent kinase 6
CCND1	cyclin D1
CMV	cytomegalovirus
DAAM1	disheveled-associated activator of morphogenesis 1
DDX1	DEAD (Asp-Glu-Ala-Asp) box helicase 1
DGCR8	DiGeorge syndrome critical region 8
DMs	double minutes
DNA	deoxyribonucleic acid
DPP	decapentaplegic
dre	*Danio rerio* (Zebrafish)
DTT	dithiotreitol
E2F3	E2F transcription factor
eIF4E	eukaryotic transcription factor 4E
EMT	epithelial-to-mesenchymal transition
FAM	carboxyfluoroscein
FBS	fetal bovine serum
FGF	fibroblast growth factor
FL1-H	fluorescence channel-1-height
FSC-H	forward scatter-height
IDT	Integrated DNA technologies
GAP43	neuromodulin *or* anti-growth protein 43
HPRT1	hypoxanthine-guanine phosphoribosyltransferase
hsa	*Homo sapiens*

HSRs	homogeneously staining regions
HuR/*ELAVL1*	Hu-antigen R/ ELAVL1 (embryonic lethal, abnormal vision)-like protein 1
INSS	International Neuroblastoma Staging System
kDa	kilo Dalton
LOH	loss of heterozygosity
MAD	mothers against dpp
MAP3K9	mitogen-activated protein kinase kinase kinase 9
MAX	MYC associated factor x
MET	mesenchymal-to-epithelial transition
MRE	microRNA recognition element
mRNA	messenger RNA
min	minutes
miRNA	microRNA
miRNP	microRNA ribonucleoprotein complex
MNA	*MYCN*-amplification
MYC	*V*-myc myelocytomatosis viral related oncogene (avian)
MYCN	V-myc myelocytomatosis viral related oncogene, neuroblastoma derived (avian)
NAG	neuroblastoma amplified gene
NF1	nuclear factor I
NF-κB	nuclear factor-kappa B
NPY	neuropeptide Y
NCCs	neural crest cells
NGS	next generation sequencing
nm	nanometer
nt	nucleotide
P-bodies	processing bodies
PBS	phosphate buffered saline
PCR	polymerase chain reaction
PDCD4	programmed cell death 4
PTEN	phosphatase and tensin homolog
pre-miRNA	precursor-microRNA
pri-miRNA	primary-microRNA
qPCR	quantitative real-time PCR
RISC	RNA inducing silencing complex
RLU	relative luciferase units
RT	real-time *or* room temperature
RNA	ribonucleic acid
SIRT1	sirtuin 1*or* silent mating type information regulation-2 homolog *or* silent information regulator 1
SPRY2	Sprouty homolog 2
DHA	succinate dehydrogenase

ss	single-stranded
SSC-H	side scatter-height
ssRNA	single-stranded RNA
snoRNA	small nucleolar RNA
STAT3	signal transducer and activator of transcription 3
TGFβRII	transforming growth factor β receptor II
TMEM49	Transmembrane Protein 49
TF	transcription factor
UTR	untranslated region
VMP1	vacuole membrane protein 1
WNT	portmanteau of Int and Wg
Wg	Wingless-related integration site

2 Abstract

Neuroblastoma is an embryonal cancer of the post-sympathetic nervous system and is the most frequent extra-cranial solid tumor in childhood. Two important microRNAs, the tumor suppressor *mir-34a* and the oncogenic *mir-21*, have been found to increase during *MYCN*-knockdown induced differentiation. However their distinct roles are not clear. This thesis employs a method to identify the mRNA targets of *mir-21* and *mir-34a* by the capture of biotin-labeled microRNA-mRNA complexes. The function of the biotin-labeled microRNA duplexes *mir-21* and *mir-34a* were proven to be biologically active by targeting of the antisense *mir-21* and *MYCN* 3' UTR cloned into the firefly luciferase, respectively. Further, these luciferase vectors were used to prove the applicability of the pull-down approach where *mir-21* and *mir-34a* enriched for their respective targets. A biotinylated, negative control did not enrich for the luciferase transcript nor did the biotinylated mimics enrich for HPRT1 (a housekeeping gene). Moreover, the method was used to search for endogenous targets in the *MYCN*-amplified neuroblastoma cell line SK-N-BE(2)c. The pull-down results of *mir-34a* yielded high enrichment of *MYCN* and *CCND1* (cyclin D1). Additionally, *SIRT1* was a probable target of mir-34a. Two mRNAs that previously were shown to be targeted by *mir-21* in human cancers, *PTEN* and *PDCD4*, were not enriched from neuroblastoma cell extracts. Previous results from our lab have also shown that *pre-mir-21* over-expression do not affect *PTEN* and *PDCD4* protein levels. Over-expression of the biotinylated *mir-21* duplex did neither affect mRNA levels of *PTEN* nor *PDCD4*. *mir-21* was as such concluded to not target *PTEN* and *PDCD4* in the human neuroblastoma cell line SK-N-BE(2)c. Moreover, *mir-34a* over-expression in BE(2)c showed a 4-fold reduction of *MYCN* and a 20 % increase in *CCND1*. Mechanisms of *mir-34a* were therefore believed to repress and perhaps direct *CCND1* to P-bodies. *mir-34a* over-expression resulted in the respective 1.75 and 7.8 fold increase of the two neuronal differentiation markers *NPY* and *GAP43*. This was conclusive with the tumor suppressing role of *mir-34a*. Additionally, the role of *mir-34a* in neuroblastoma is discussed in detail. Concluding, this thesis demonstrates how biotinylated microRNA duplexes can be used to identify miRNA-mRNA targets.

3 Introduction

3.1 Neuroblastoma

Neuroblastoma, accounting for 7-10 % of pediatric cancers, is thought of as an embryonal cancer of the post-sympathetic nervous system[1, 2]. It is the most frequent extra-cranial solid tumor in childhood representing 7-8 % of all pediatric malignancies and 15 % of childhood cancer deaths[2, 3]. Regression of cancer tumors are not as clearly seen as they are in neuroblastoma, implying that the developing child's cells are able to turn off the proliferative state of neural crest cells (NCCs). In comparison, neuroblastoma has a 10 to 100 fold greater spontaneous regression rate than any other type of cancer. These regressions are most abundant in low risk grade tumors such as stage 1-2 and 4s (see Figure 1 for a more detailed overview of stage 1-4 and 4s in the International Neuroblastoma Staging System[4, 5]). However, patients with high risk grade (stage 4) tumors have also been proven to show spontaneous regression[6]. As a general outline, the presence of *MYCN* amplification and/or prolonged half-life of the *MYCN* oncogenic transcription factor correlate with advanced stage tumors and little chances for regression[7]. As such, treatment of high-risk neuroblastoma patients remains a major challenge with a survival rate below 40 %[8-10].

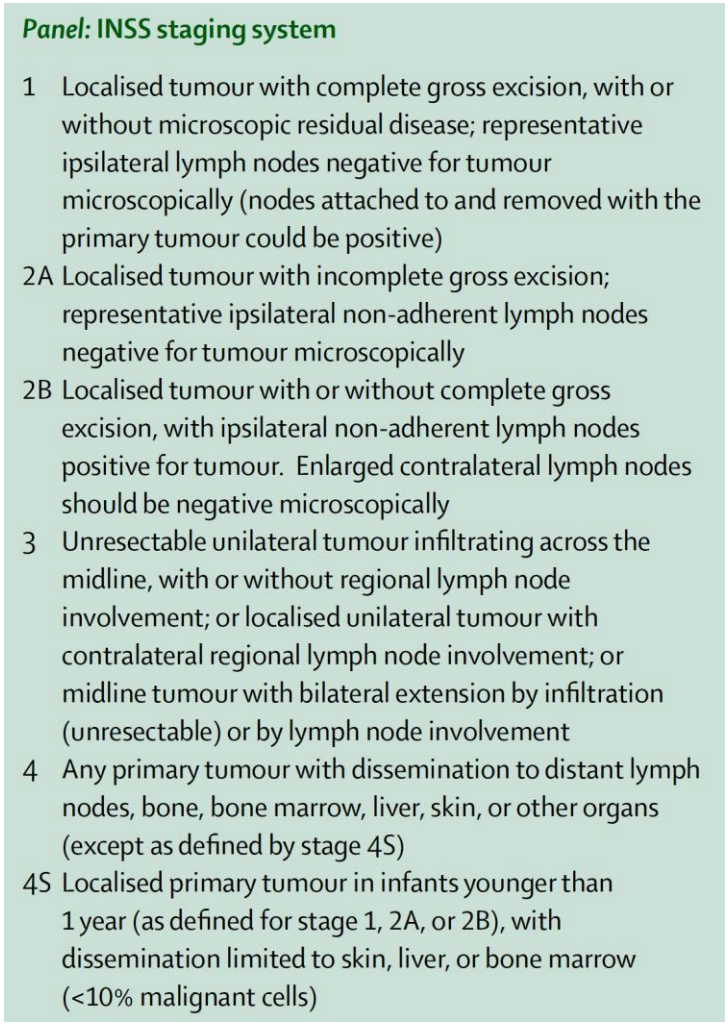

Figure 1 | The International Neuroblastoma Staging System (INSS)[4, 5]. Classification according to localized (stage 1-2), locoregional (stage 3), metastatic tumor (stage 4) and tumors with a high capability of showing spontaneous regression (stage 4s).

The sympathetic ganglia arise from trunk NCCs that migrate through a ventromedial pathway along the neural tube. During this migration, they migrate through the rostral part of each somite and encounter spatiotemporal cues from the surrounding environment. These cues include signals from all three embryonal layers: ectoderm (neural plate, neural tube, skin), mesoderm (notochord, somites) and endoderm (gut, liver, lungs). In short, these signaling pathways comprise of Hedgehog, *BMP*, *FGF*, *WNT* and *PHOX2B*. Depending on the cellular environment, NCCs will differentiate into melanocytes, Schwann cells and neurons. During the migration of NCCs, signaling defects (concentration gradient, mutations, chromosomal aberrations) can result in the formation of neuroblastoma. Prognostic factors important in neuroblastoma comprise especially of *ALK* and *MYCN*

mutations[11]. However, more factors are needed to convey the clinical and molecular picture of neuroblastoma heterogeneity as well as other cancers to being able to find prognostic factors that can either serve as a tool for diagnostics or that can be targeted using therapeutic drugs. The experimental procedure outlined in this thesis can aid in finding these factors. It can also be applied to pinpoint the importance of some microRNAs during the migration of neural crest cells during human development and neurulation.

3.1.1 The MYCN oncogene and MYCN-amplification in neuroblastoma

The *MYCN* oncogene is located on chromosome 2p24 and encodes the 49.56 kDa N-Myc oncoprotein. N-Myc, an important transcription factor in embryogenesis, localizes to the nuclear matrix, and has a short half-life of 30-50 min. It is normally expressed in the developing embryo and various proteins with a basic helix-loop-helix (bHLH) domain bind to N-myc [12]. The general aspect of neuroblastoma is that whenever *MYCN*-amplification occurs in patients, the survival drastically decreases as a result of poor prognosis and often metastatic disease. This is independent of age and stage diagnostics. Also, *MYCN* gene amplification has been identified in a broad range from 50 to 500 copies of the gene per cell. Intermediate copy level numbers (3-10) are usually a result of low level duplications or aneuploidy, and often reflect lower risk stages. *MYCN*-amplification (MNA) is predominant in 20 % of neuroblastoma tumors[13]. Other genes found to be co-amplified with *MYCN* (<50 %), are *DDX1*[14-16] and neuroblastoma amplified gene, *NAG*[17]. Whether these genes have any molecular importance is not clear. The process of amplification seem to be occurring when small circular DNAs called double minutes (DMs) are generated and integrated linearly as homogeneously staining regions (HSRs). *MYCN*-amplification does not necessarily need to happen through gene amplification (DMs and HSRs). Other processes beyond the genomic level can increase the level of *myc* transcription factors. Among these may be attenuated ubiqutilation and protein degradation, regulatory RNAs, the importance of the N-end rule (N-end terminal portion of the translated protein determinates its half-life[18]), mRNA prolonged half-life[19], promoter expression and epigenetics. Another system that complicates *myc* levels is the Mad:Max network. Max is able to form homodimers and heterodimers with other members of the basic helix-loop-helix leucine zipper (bHLHLZ) family, which includes myc proteins, Mad1, Mad3, Mad4, Mxi1 (MAX-interacting protein 1), Miz, Mnt, and Mga[20-24]. The different homo- and heterodimers all compete for the

transcriptional implicated site found internally in promoter regions, termed the E (enhancer) box. Max proteins are obligate dimerization partners to myc proteins binding to E-box motives during transcriptional activation of gene expression. Myc interactions with other proteins of the bHLHLZ transcription family can regulate retention or progression through the cell cycle clock by affecting positive or negative regulators such as cyclin dependent kinases (CDKs), cyclins and proteins involved in proteolytic degradation of different cell cycle regulators. Myc also recruits histone deacetyltransferases, thus turning on transcription of many genes by regulating the global chromatin structure. Myc also turns on the transcription of several microRNAs, including the *mir-17-92* cluster[25]. Ultimately, myc may regulate the transcription of hundreds, if not thousands of genes.

3.2 RNA vs DNA

The fundamental difference between RNA and DNA is that RNA contains 2' hydroxyl (OH) group. By adding this group, RNA molecules have a higher melting temperature (T_m) and stability by locking the RNA duplex into a compact A-form helix that is more stable and shorter than the B-form helix adopted by DNA molecules. This structural difference accounts for the formation of different helical grooves that create very different surfaces for protein binding. RNA is able to form self-folding structures such as pri-miRNA (discussed later). These self-forming structures form an RNA duplex/helix with van der Waals interactions between neighboring bases in the same strand as well as to complementary bases that stabilize the structure. The folding structure depends on base composition, their interactions with each other and with ribose sugars, phosphate groups and with the surrounding environment (ions, proteins, etc.). The base interaction is of course dependent on the bases themselves, as such it should be mentioned that RNA molecules are post-transcriptionally modified with pseudouridine, 2'-O-methylation of the ribose ring, and base methylations at various positions. Thus, the bases found in RNA are numerous compared to DNA, and to date more than 100 different nucleotides have been identified (*e.g.* 4-thiouridine, 6-thioguanine and 7-iodouridine) . In the advent of next-generation sequencing (NGS), Morin found a number of miRNAs showing RNA editing (isomirs)[26]. As a result of post-transcriptional modification of RNA, mimicking miRNAs and

endogenous miRNAs may be utterly different and display different properties in respect to mRNA targeting and one should have this in mind when working with artificial produced RNA molecules.

3.3 miRNAs

MicroRNAs (miRNAs) are short (18-24 nucleotides) RNA molecules that belong to a family of small regulatory, noncoding RNAs which base-pairs to target mRNAs to induce post translational repression in mammalian cells. Typical traits of miRNA expression in tumorigenesis are that some of the developmental/embryological stage miRNA are turned constitutively on. These in turn may increase the proliferation rate and may also deregulate the differentiation of NCs. Another key that implicates RNA regulation, are the RNA editing mechanisms which may turn on and off expression both on the transcriptional and translational level. They are considered to have an equal amount of responsibility as transcription factors (TFs) in altering the population of messenger RNAs. As TFs, miRNAs can be considered as both tumor promoters (oncomirs) and tumor suppressors. As such, understanding the maturation and function of miRNAs is essential for *in vitro* and *in vivo* studies. According to miRBase release 19 (May 2013)[27-30], 1600 precursor and 2042 mature miRNA sequences are now present in the human genome[31]. The number of miRNAs will undoubtedly increase in huge numbers with the application of next generation sequencing (NGS). A huge issue in microRNA regulatory networks, is that miRNAs may target several hundreds to thousands of mRNAs and mRNAs themselves may contain several to hundreds of microRNA recognition elements (MREs). MREs are most commonly found in the 3′ UTR region of mRNAs, but may also reside in other sites of mRNAs, *i.e.* CDS and 5′ UTR[32, 33]. Normally, a scientist would employ a gene knockdown study combined with a luciferase based approach to investigate a putitative target. Using this approach would only allow the scientist to validate the target by its MRE cloned into the luciferase reporter, where the 3′ UTR being used as the MRE in nearly all of the occurrences. Using another approach with biotin tagged miRNAs, as outlined in this thesis, shows a more reliable and efficient approach to find miRNA targets in respect to the MRE's genomic location. Here, tagged miRNA mimics are introduced into the cell and miRNA-mRNA complexes are affinity purified using streptavidin beads. The captured mRNA population is

dissociated from the bound miRNA complex and analyzed by qRT-PCR to detect the putative targets. A higher presence of a target's transcript pull-down:input ratio signifies a higher probability that it is a direct target of the introduced miRNA.

3.3.1 Biological synthesis of miRNAs

Different factors and pathways are important in the synthesis of mature miRNAs. In all scenarios, miRNAs function as specificity determinants whereas Ago proteins perform the silencing effect during mRNA suppression. To date, the location of miRNA in the human genome has shown to be varied. The vast majority of miRNAs in mammalians are found within introns of protein coding genes[34], whereas some are found in introns and/or exons of long-noncoding RNAs. A recent event showed that *mir-664*, *mir-1248*, *mir-1291* have shown to be encoded within snoRNA (small nucleolar RNA) of ACA36B, HBI-61 and ACA34, respectively[35]. This suggest that the maturation of some miRNAs may be related to that of snoRNAs, a class of small-noncoding regulatory RNAs (60-300 nt) that serve as guides for the catalytic modification of ribosomal RNA[36, 37]. In the canonical miRNA processing pathway, RNA polymerase II produces primary miRNA (pri-miRNA) transcripts from long mono- or polycistronic transcripts that can vary in size (~150 nt)[38-40]. The pri-miRNA is processed by the RNase III enzyme Drosha in complex with co-factor DGCR8 generating a ~70nt transcript which is now termed pre-miRNA (precursor-miRNA). This is exported out of the nucleus via exportin-5 through binding to a 2 nt 3′ overhang generated by all RNase III family proteins [41, 42]. In the cytoplasm, the pre-miRNA is further processed by Dicer which cuts the pre-miRNA an exact length from the phosphorylated 5′ end[43]. After cleavage to generate the mature miRNA duplex, it is further loaded to Ago, the core component of the silencing machinery in mammals. It has been shown that all Ago proteins are present in humans (Ago 1-4) and that all of them have the capability of gene silencing when a particular miRNA is overexpressed[44, 45]. miRNAs have found to degrade and cleave their targets in plants by perfect complementarity[46]. In humans, the scenario is different and the outcome of miRNA-mRNA base pairing decides the fate of mRNA. Here, an important region called the bulge region impairs the catalytical activity of Ago2, hence translational repression is the fate of the mRNA rather than degradation. The mature miRNA (sense strand) together with its argonaute protein confers its effect in the RNA Inducing Silencing Complex (RISC) where miRNA-mRNA target cleavage or translational repression occurs.

miRNAs can also bypass cleavage by Drosha (mirtrons). Here, miRNAs overlap with exon-intron junctions and mature through alternative splicing.

3.3.2 Structure and target recognition of miRNAs

The sequence of the miRNA decides the fate of the target as mentioned in the previous paragraph. It has been shown that miRNAs possess evolutionary conserved sequences from species to species. Several rules have been proposed to affect the base pairing of miRNAs to its target[47-51]. Three rules are essential for miRNA silencing: (1) seed rule comprising the hyperconserved nucleotides 2-8 (shown in dark red and green) accounting highly for the miRNA-mRNA association. Often, this is the region which is mutated when experiments require abolishing of the miRNA-mRNA association. Additionally, the seed region varies from miRNA to miRNA. The canonical seed region includes the 7mer-A1/m8 site. Here, nucleotides position 2-7 and an A at position 1 and/or a match at position 8 greatly increase the efficacy of pairing to the target mRNA. An A or U at position 9 also improves site efficiency. Another rule is that the 3′ complementarity region must stabilize the interaction. Here, residues 13-16 have found to be the most conserved and thus is most important for the stabilization of the microRNA paired to its MRE. Other important factors that contribute to the stabilization, is the MRE and the regions in close vicinity[50-52]. For instance, would an MRE residing in the CDS region of the mRNA be more accessible if it has fewer ribosomes (as would be expected by other types of repression such as the N-end rule). Another proposal is that MREs residing in the UTR region accompanied by flanking regions of high AU content would give a lesser degree of binding to RNA binding proteins or a lower degree of RNA tertiary structure, thus making the miRNA more readily accessible to target the MRE.

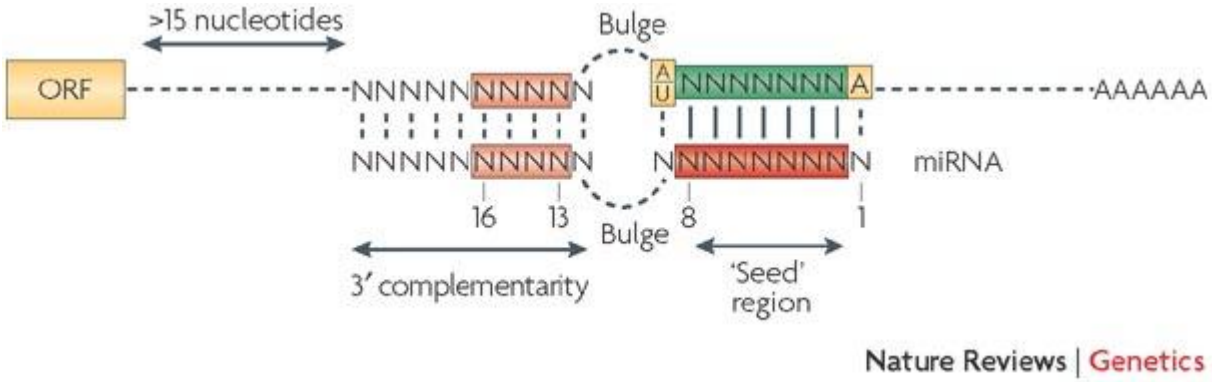

Figure 2 | Important regions for miRNA-mRNA interaction[46]. In humans, miRNAs with partial complementarity induce mRNA repressional translation. The amount of complementarity depends on the seed region and 3' complementarity region. Another important region, the bulge region, prevents argonaute proteins from breaking the mRNA strand in two. Without the bulge region, the outcome is tended towards mRNA degradation which is more common in plants and lower species[32, 47-49, 53].

3.3.3 Role, function and impact of miRNAs

A multitude of mechanisms of how miRNA regulates the pool of mRNA molecules in the cell have been proposed. These are summarized below where deadenylation, proteolysis, initiation block and elongation block are some of the ways miRNAs exert their function. It has also been shown that miRNAs can direct their target to P-bodies for mRNA storage or degradation. Mechanisms proposed to undergo in P-bodies are mRNA decapping and degradation, storage until needed for translation and aiding in translational repression of miRNAs.

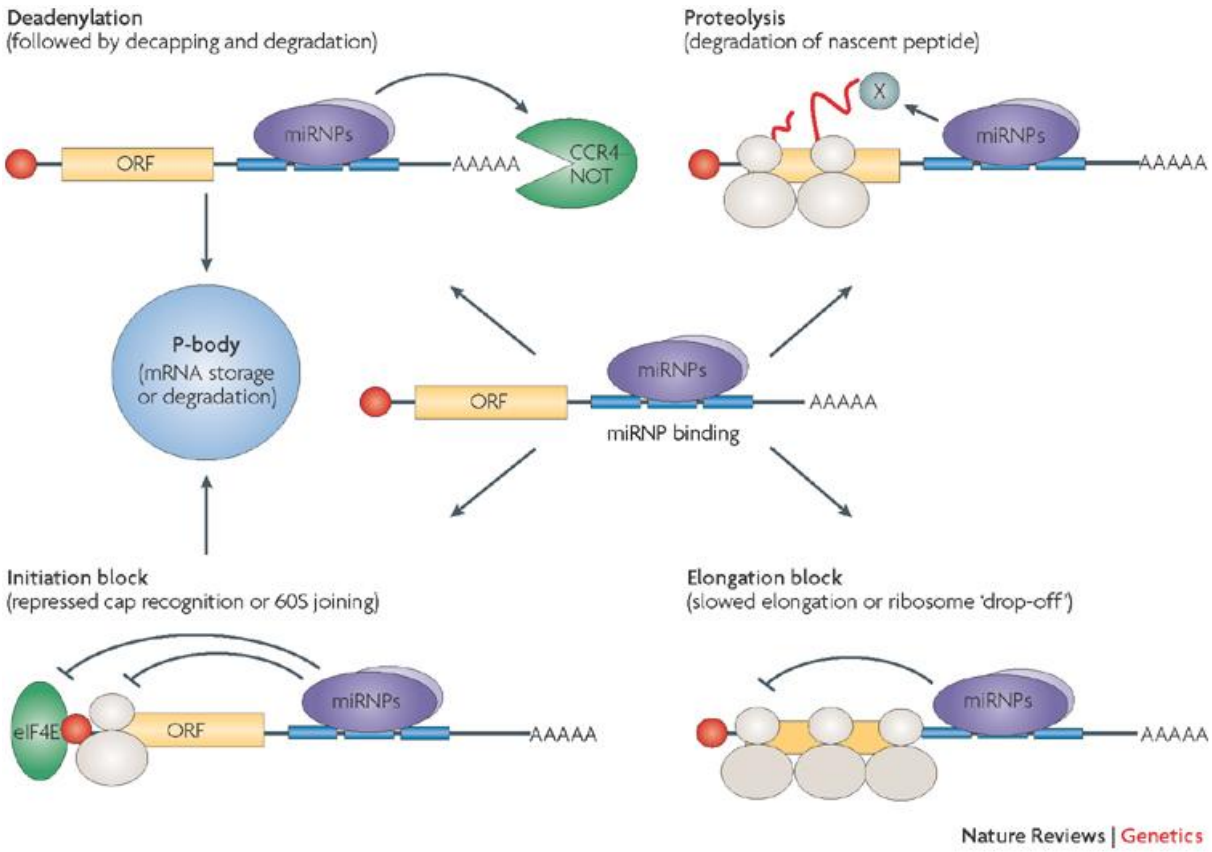

Figure 3 | Mechanisms of post-transcriptional regulation by microRNAs[46]. miRNA-mRNA binding (middle) can cause (1) deadenylation and subsequently degradation by exonucleases such as CCR4-NOT[54, 55], (2) initiation of proteolysis by the nascent peptide[56], (3) preventing recognition of the 5' cap structure[57, 58] or 60S joining of the ribosome[59] and entry to the mRNA molecule leading to an untranslated mRNA molecule, and (4) elongation block where the mRNA molecule's translation is slowed or the ribosome drops off[60], thereby preventing the full-length of the mRNA molecule to be translated. miRNA-mRNA complexes have found to be stored in intracellular P-bodies in complex with Ago-2. eIF4E, eukaryotic initiation factor 4E. The 7-methylguanosine cap is shown as a red circle.

3.4 Approaches for miRNA-mRNA target exploring

As with transcription factors, miRNAs can regulate gene expression in a myriad of ways. As of today, the substantial amount of miRNAs (not to even mention isomirs) that exist has yet to be fully mapped to their mRNA targets for being able to understand systems biology. Systems biology does not only contain intracellular signaling, but also intercellular signaling from different cell types, even from completely different organs. For instance, microRNAs have been shown to be exported within exosomes to stromal cells in the tumor environment. This form of export may be a way of the tumor to manipulate its

environment in case of angiogenesis, self-sustaining growth by manipulating the adaptive immune system, etc. This complexity is a speed brake for developing therapeutic and diagnostic approaches to diseases and cancers such as neuroblastoma. By using biotin-labeled microRNAs and streptavidin-coated magnetic beads, this thesis explores how miRNA-mRNA targeting occurs on the endogenous mRNA inside cells as opposed to the standard luciferase procedures that have been previously used to validate target mRNAs. As opposed to finding miRNA-mRNA targets by *in silico* analysis and further validate the targeting by luciferase experiments, the pull-down applied in this method shows that it is a robust and an effective method of finding targets of *mir-34a*. A profound advantage here is that these assay have the opportunity to present the scientific community with both validated and novel targets such as previously shown with *miR-1* in *Danio rerio*[61], *mir-34a* in HCT116 colon carcinoma and K562 erythroleukemia cells[62], and isolation of *bantam* miRNA-*luc hid* complexes in HEK-293 cells[63]. Other protocols that have been used to investigate miRNA target identification are reviewed by Thomson *et al.* 2011[64]. Some of the approaches listed here are Argonaute high throughput sequencing of cross-linking of immunoprecipitation (HITS-CLIP or CLIP-Seq)[65] , photoactivateable-ribonucleoside-enhanced crosslinking and immunoprecipitation (PAR-CLIP)[66], and reverse transcription of targets where miRNA are used as primers for the cDNA synthesis[67, 68]. Other analysis relies on widespread transcriptome (microarray, NGS) or proteome profiling (stable isotope labeling with amino acids in cell culture or SILAC) after the introduction of exogenous miRNA. In the biotin tagged miRNA technique applied in this thesis, the experimental procedure can be explained briefly by (a) introduce the cell with a tagged biotin miRNA and then (b) pull-out the biotin-microRNA-mRNA complex by using magnetic streptavidin beads which show one of the strongest known noncovalent, biological interaction known (*K*d in the order of 10×10^{-14} M)[69]. The bond forms very rapidly and is stable across a range of pH and temperature[70].

3.5 mir-21

mir-21, found at 17q23.2 and overlapping with *VMP1* (*TMEM49*), is matured from *pre-mir-21* that is several kilobases in length[71] and is found in an region that is frequently altered in neuroblastoma and is associated with poor prognosis[72]. The first sights of *mir-21* revealed it

as an anti-apoptotic factor in glioblastoma[73]. *mir-21* have been found to be upregulated in cancers such as breast cancer[74, 75], glioblastoma[76, 77], hepatocellular carcinoma[78], cholangiocarcionoma[79], pancreatic cancer[80], renal cell carcinoma[81] and numerous other cancers. Targets that are previously identified for *mir-21* are PTEN[82], PDCD4[83], FasL[84, 85], SPRY2[85, 86], and TGFβRII[87]. Previous reports show that the promoter region of *mir-21* binds *AP-1* (comprising Fos and Jun), Ets/PU.1, *C/EBP-α*, *NFI*, p53 and *STAT3*[88]. In a recent paper published by our research group, *mir-21* expression was found to be reverse correlated to *MYCN* expression during induced neuronal differentiation of *MYCN*-amplified neuroblastoma cells. No targets for *mir-21* were identified in this study[89].

3.6 mir-34a

LOH of 1p36 is a deletion found in 25-30 % of all cases in neuroblastoma and is associated with poor prognosis[90-92]. Interestingly, this genomic aberration is also found in brain tumor, melanoma, leukemia, breast cancer and cervix cancer[93-97] implying that this region harbors important tumor suppressing functions. Genomic experiments have found to identify *mir-34a* as one of these tumor suppressors, capable of targeting *MYCN*, a known oncogene and reverse correlated with *mir-34a*[98, 99]. Other targets that have been proposed for *mir-34a* are *MYCN*[98], *CCND1* (cyclin D1)[62, 100], *MAP3K9* (failed to demonstrate direct targeting by luciferase assay)[101], *CDK4*[62], *CDK6*[100], *E2F3*[62], *PDCD4* (TargetScan 6.2), *DAAM1* (TargetScan 6.2), and *SIRT1*[62, 102]. However, these *mir-34a* targets have not been validated in neuroblastoma. Additionally, HuR have shown to reverse correlate with *mir-34a* expression[103]. The promoter region of *mir-34a* has been shown to be a target of p53[104] and *NF-κB*[105]. p73, a p53-related tumor suppressor, resides in the vicinity of *mir-34a* (in 1p36.1 and/or 1p36.3). It has previously been shown that SK-N-BE(2) is monoallelic for p73 and express very low levels of p73 and no protein., suggesting that SK-N-BE(2)c is also monoallelic for *mir-34a* (1p36.23) as it encompasses very low expression of *mir-34a*.

4 Aims

The role of miRNAs in cancer has been shown to exert a tremendous amount of roles both in regards to suppressing and driving the cell into a tumorigenic state. Understanding the role of miRNAs is therefore imperative to unravel the mystery and the underlying mechanisms of such disorders. As such, the main aim of this thesis was to establish a method for finding miRNA-mRNA targets for *mir-34a* and *mir-21*. In extent, the thesis addressed the following:

1. **Produce an in-house, simple, direct, reliable and cost-effective method for finding microRNA-mRNA targets.**

   The thesis presents with a technique that reliably identifies microRNA targets. The method was optimized and pull-down results from this thesis represented results that were consistent with the literature. As such, the results conclude that this is a valid approach for detecting miRNA-mRNA targets.

2. **Understand the tumor suppressing role of *mir-34a* in neuroblastoma.**

   mir-34a has been shown to act as a tumor suppressor in a variety of cancers. The role of *mir-34a* has to a small extent been investigated in neuroblastoma. Here, the *MYCN*-amplified cell line SK-N-BE(2)c was used to investigate targets of *mir-34a* which was shown to target *CCND1* and *MYCN*. *CCND1,* as opposed to *MYCN,* have previously not been validated as a target in neuroblastoma. Both targets confer the tumor suppressing effect of *mir-34a*. *MYCN* was also validated as a target by luciferase experiments where the 3' UTR was cloned into the pCMV firefly reporter vector. *SIRT1* was also shown to be a target of *mir-34a*.

3. **Understand what function *mir-21* elicits in neuroblastoma**

   As previously shown by our research group, *mir-21* and *MYCN* expression is strongly reverse correlated during neuroblastoma *MYCN*-knockdown induced neuronal differentiation[89]. This suggests that *mir-21* plays an important role in neuroblastoma tumorigenesis. However, the role of *mir-21* has previously not been described in

neuroblastoma. *mir-21* was found to not target *PTEN*, *PDCD4 and TGFβRII*. Further investigation of *mir-21* is necessary to identify its targets in neuroblastoma.

5 Materials and methods

5.1 Cell lines

SK-N-BE(2)c (a stage IV cell line, del(1)p, monosomy 17, and unbalanced der(3)t(3;17), HSRs of *MYCN* in 6p and 4q[106, 107] and low/absent expression of *mir-34a*[108] as suspected by the reverse correlation with *MYCN*[98]) and SK-N-AS (a stage IV cell line, expressing *mir-21* at intermediate levels and 40 % higher than SMS-KCN[89], 1pdel and only a single copy of *MYCN*[109]) were used in the following experimental procedures. Both cell lines were grown in RPMI-1640 supplemented with 10 % FBS at 5 % CO_2 with air at 37°C for one day to reach 30-50 % confluency at the time of transfection (as recommended by the manufacturer's protocol). BE(2)c was used in all experiments except for the luciferase and luciferase pull-down of *mir-34a* and *mir-21*. Cells were harvested after reaching 80-90 % confluency two days after transfection.

5.2 Designing biotinylated miRNAs

Duplex miRNA mimics (IDT) was ordered separately as two single strands with the guide strand having the attached 3'-biotin. Each strand was reconstituted to 100 µM and mixed in a 1:1 ratio, thereafter hybridized by heating to 80°C and cooled down on ice. The underlined base in the passenger strand of *mir-21* was mutated from the original cytosine to uracil creating a G:U wobble and a less thermodynamically stable mimic. This is hypothesized to enhance the incorporation of the guide strand into RISC[110]. The negative control mimic was designed with 3'-end labeling of the guide strand *cel-mir-67-3p* and hybridized to the passenger strand. All miRNA sequences were obtained from miRBase release 19.

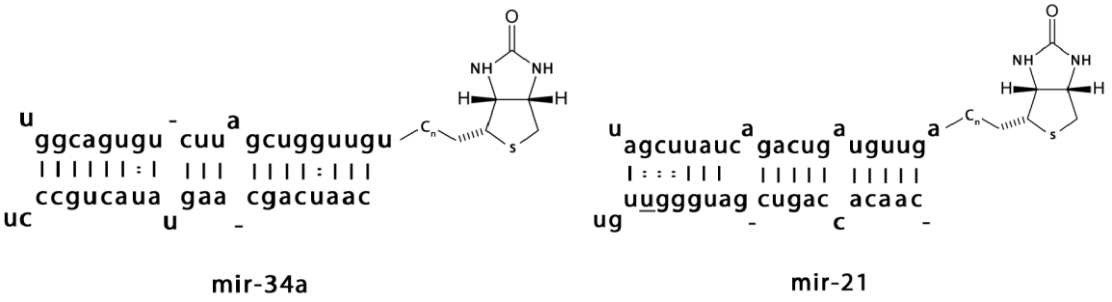

Figure 4 | Schematic representation of *mir-34a* and *mir-21* duplex with 3'-biotin used in this thesis. | and : represent GC/AU base-pairing and GU wobbles, respectively. C_n represents the spacer arm between the 3' end of the guide strand and the biotin molecule. Sequences were obtained from miRBase.

5.3 Establishing transfection conditions by flow cytometry

For testing transfection efficiency with Lipofectamine 2000, 130 000 SK-N-BE(2)c was seeded in a 6-well plate. One day after seeding, two wells were transfected with 75 pmol NC FAM (*Caenorhabditis elegans mir-67* with 3'-end-labeled 6-carboxyfluoroscein). Background fluorescence was set by transfecting two wells with 75 pmol bi-*cel-mir-67*. 48 hours after transfection, cells were trypsinated and diluted to 0.7 ml in RPMI-1640 supplemented with10 % FBS. Immediately after, cells were filtered and run on FACS Calibur to test the amount of cells that have acquired the FAM labeled mimic. 15 000 events were registered for the transfection efficiency test.

5.4 Transfection conditions for capturing bound luciferase constructs

SK-N-AS was seeded with 80 000 cells in a 6-well plate with four replicates per pull-down. One day after seeding, each well was co-transfected with 75 pmol biotinylated, duplex miRNA (bi-*mir-21* or bi-*mir-34a*) and 300 ng of report vectors (pCMV-FL-21-as or pCMV-FL-MYCN3'UTR). After two days the cells were harvested and RNA was Trizol isolated and analyzed by RT-qPCR.

5.5 Pull-down transfection conditions

SK-N-BE(2)c was seeded with 130 000 cells in a 6-well plate with four replicates per pull-down. One day after seeding, each well was transfected with 75 pmol of duplexes using 3

µl Lipofectamine 2000 (Invitrogen) diluted in Opti-MEM Medium. After two days, the replicates were harvested and pooled together to yield a satisfying amount of mRNA input to the cDNA reaction. cDNA from the pull-down and input samples was analyzed by qPCR. Typically, the expected yield from the pull-down using this transfection protocol were 100-300 ng of mRNA assessed using nanodrop.

5.6 Luciferase

For ensuring that the biological function of the mimics are intact, 80 000 SK-N-AS cells were seeded in a 12-well plate and transfected one day after seeding. 100 pmol biotinylated miRNA mimic was co-transfected with 20 ng of pCMV Renilla (*Renilla reniformis*) luciferase vector (Promega) and 100 ng firefly (*Photinus pyralis*) luciferase report vector. The firefly luciferase reporter vectors contain miRNA targets in the 3'UTR of the luciferase mRNA and is used to assay the effect of miRNA gene repression. The Renilla luciferase reporter constitutively express the Renilla mRNA and is used for normalization. Moreover, to assess whether or not the addition of biotin to the mimics would have any profound effect on its biological function, mimics without biotin were co-transfected with the same amounts of firefly and Renilla report vectors. The anti-sense sequence and the MYCN 3' UTR was cloned in the 3'UTR of the luciferase reporter and used as means to reflect the biological activity of *mir-21* and *mir-34a*, respectively. Both vectors were validated by sequencing. Two days after transfection, luciferase was measured using the Dual Luciferase Kit (Promega). Each well was washed with 1 ml 1x PBS and lysed by shaking at 150 x rpm with 125 µl Passive Lysis Buffer (Promega) for 15 min. Relative luciferase units were measured on Luminoskan Ascent (Thermo Scientific) by using 20 µl lysate, 50 µl LARII and 50 µl Stop&Glo. Integration and lag time was set to 10000 and 2000 ms, respectively.

5.7 Pull-down of direct targets of *mir-34a* and *mir-21*

Cells that have grown for 48 hours after transfection and reached a confluence of approximately 80-90 % were washed with PBS, trypsinated and resuspended in RPMI-1640 supplemented with 10 % FBS. Cells were harvested using a cell scraper and moved to a microcentrifuge tube, spun down at 500 x for 5 min at 4°C and washed with 1 ml 1x PBS.

The cell pellet was lysed with 350 µl filter sterilized, cell extract buffer (25 mM Tris pH 8, 100 mM KCl, 5 mM $MgCl_2$, 0,3 % NP-40, 50 U RNasin (Ambion), Roche complete mini protease inhibitor cocktail in DEPC-treated H_2O) for 10 minutes on ice. The lysates was spun down at 10 000 x G for 10 min at 4°C to remove cellular debris and nuclei. This step is important to enhance the binding of mRNA targets to the biotinylated mimics. After centrifuging, a 5 % input was stored for later Trizol isolation of RNA and the remaining supernatant was used for pull-down. Streptavidin M-270 Dynabeads (Invitrogen) was pre-blocked for 2 hours with rolling at 4°C with a final concentration of 1 mg/ml yeast tRNA (Ambion) and 1 mg/ml BSA (New England Biolabs). Before the beads was applicable for pull-down, they were washed twice with 1 ml cell extract buffer and resuspended to 1/3 of the initial volume (30 µl) taken out of the Streptavidin M-270 vial. The remaining 332.5 µl cell extract was mixed with 10 µl pre-blocked beads and incubated at 4°C with rolling for 3 hours to capture miRNA targets, and thereafter washed 5 times with 1 ml cell extract buffer. After the last wash, the beads were moved to a new tube and resuspended to 50 µl with cell extract buffer before proceeding to Trizol isolation of RNA. The Trizol isolated RNA was used in RT-qPCR.

5.8 Over-expression and knockdown of mir-21 and mir-34a targets

mir-21 and *mir-34a* mimics, both biotinylated and non-biotinylated, were transfected at 100 pmol into SK-N-BE(2)c. Cells were grown for two days after transfection and RNA was isolated using Trizol (Invitrogen). After Trizol isolation, RNA was post-forwarded to RT-qPCR.

5.9 Trizol isolation and DNase-treatment of RNA

1 ml of Trizol (Invitrogen) was added to the samples, vortexed for 1 minute and placed at RT for 5 min before adding 200 µl chloroform. The phases were mixed and phase separation was done by centrifuging at 12 000 x G, 15 min at 4°C. To maximize yields and reducing the risk of phenol contamination, the lower phenol phase was removed and the sample was re-spun at 12 000 x G, 15 min at 4°C. The aqueous phase was moved to a new tube with 45 ug glycogen (Ambion) and 1 volume of 1 M NH_4OAc isopropanol. The mixture

was chilled at -20°C for 15 min and RNA was co-precipitated with glycogen by centrifuging at 12 000 x G, 15 min, 4°C. The visible RNA pellet was washed in 1 ml 75 % ethanol and reacquiring of the pellet was done by spinning down at 7500 x G, 5 min at 4°C. The pellet was resuspended in RNase-free H_2O and DNA was removed by DNase treatment using Heat-Labile Double-Strand Specific DNase (Arctic Enzymes). For DNase treatment, 0.1 U HL-dsDNase, 3 mM $MgCl_2$, 20 mM Tris-HCl (pH 8.0) and 1 mM DTT was added per µl RNA prep. Contaminating DNA was removed by incubation at 40°C for 15 min and the heat labile recombinant enzyme was heat inactivated at 55°C for 15 min. Prior to removing DNA, the A260/A280 ratio was measured on NanoDrop 1000 (ThermoScientific). DNase treated RNA was subsequently used in RT-qPCR.

5.10 RT-qPCR

RNA was reverse transcribed using High Capacity Reverse Transcription Kit (Applied Biosystems). 10 µl RNA prep was mixed with 10 µl of cDNA reverse transcription master mix following the standard protocol. RNA was reverse transcribed using the PTC-200 Thermal Cycler and using the following thermal cycling profile: (1) pre-incubation at 25°C for 10 min, (2) reverse transcription at 37°C for 120 min and (3) inactivate the reverse transcriptase by heating to 85°C for 5 min. qPCR was carried out with SYBR Green (Applied Biosystems) on the 7300 Real Time PCR System (Applied Biosystem). For each reaction, 5 µl cDNA was mixed with 15 µl SYBR Master Mix containing 10 µl SYBR, 0.8 µl primer and 4.2 µl nuclease free water. Thermal cycling was set for a 20 µl reaction with data collection at each cycle where the strands annealed at 60°C. It is important that data collection is set at this step as SYBR Green detection depends on the fluorescence of dsDNA. The complete cycler profile was (1) pre-incubation at 50°C for 2 min, (2) heat denaturation at 90°C for 10 min, (3) 40 repetitions of 95°C for 15 seconds (denaturation step) followed by data collection at 60°C for 1 min (annealing step), and (4) to validate each primer pair, a dissociation stage for each plate was applied by using 95°C, 15 sec; 60°C, 1 min; 95°C, 15 sec; 60°C, 15 sec. The cycle threshold and the baseline were set according to the7300 manual. All primers are listed in Supplementary table 2.

5.11 Percent input calculation

To calculate the amount of pull-down, this thesis apply a new way of calculating the results by using the percent input method on the results imported from the 7300 Real Time machine. The log 2 value (4.32) of the dilution factor (20) of the input sample was subtracted from each input CT. This adjusted CT was then subtracted from the pull-down CT. Finally, this number was multiplied by 100 to yield the percent pull-down relative to the input sample. Summarized, this formula applies to this calculation:

$$\% \text{ input} = 100 \bullet 2^{(\text{adjusted CT of input} - \text{CT of pull-down})}$$

, where adjusted CT of input is the original input CT value subtracted by $\log_2$ of the dilution factor

6 Results

6.1 Establishing miRNA mimic transfection conditions

In order to establish whether the neuroblastoma cell line SK-N-BE(2)c (BE(2)c) was able to take up a satisfying amount of mimic using the transfection reagent lipofectamine 2000, a fluorescent labeled negative control miRNA mimic (NC FAM mimic) which do not target any mRNAs, was transfected into BE(2)c. Further, flow cytometry of the fluorescent NC FAM mimic was used to establish whether uptake had been successful or not. Previous papers have been citing 30-50 nM as the optimal amount[62, 63]. In this study, 30 nM in 2.5 ml (75 pmol) was used to confirm high transfection efficiency. Results in Figure 5 reveal that 87.5 % of emitted light was exited from the NC FAM transfected cells by measuring the height of the FL1 pulses (FL1-H). This indicates that roughly 9/10 of the cellular population is transfected and contains the miRNA mimic. The established transfection condition was applied in the pull-down.

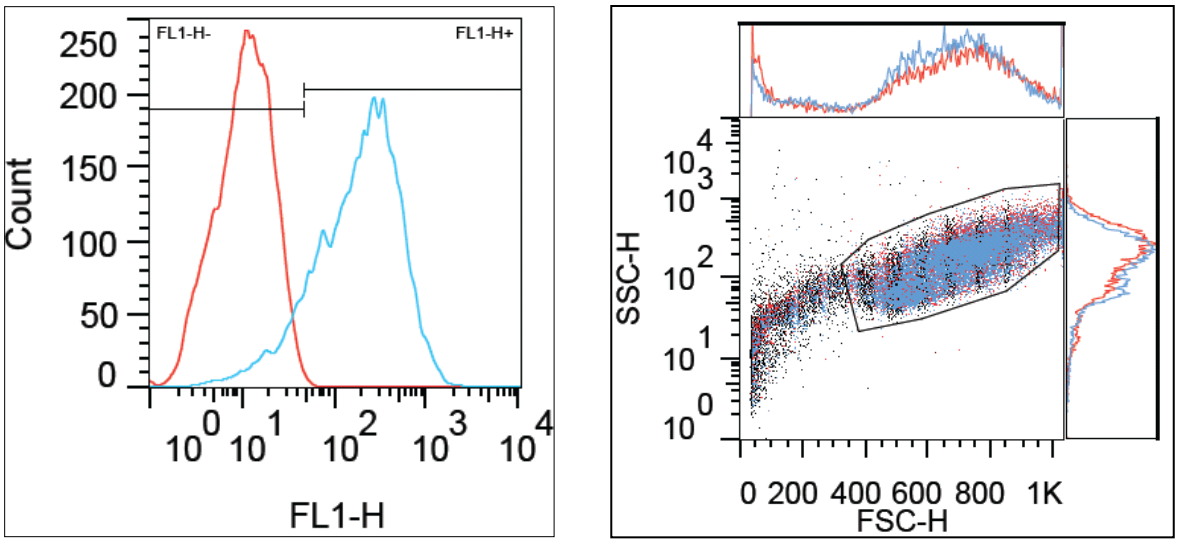

	FSC-H, SSC-H subset (%)	FL1-H- (%)	FL1-H+ (%)
NC	78.9	99.7	0.296
NC FAM	83.3	12.1	87.5

Figure 5 | Neuroblastoma cell line BE(2)c is easily transfected with miRNA mimics. FSC-H vs SSC-H dot plot (upper right) and event counts vs FL1-H histogram (upper left) of SK-N-BE(2)c was created using the FlowJo software after flow cytometry analysis on the FACS Calibur flow cytometer. Gating of the cellular population was done on NC (non –labeled FAM) mimic by using the FSC-H vs SSC-H dot plot (red population, upper right). This gated population was used to set the cut-off for cells containing NC FAM mimics (upper left). The population of both samples showed similar morphology as shown with SSC-H and FSC-H dot plot. NC FAM labeled cells showed a great shift in the FL1-H emission spectrum, and NC FAM labeled mimics was shown to be present in 87.5 % of the gated cell population (FL1-H+ of NC FAM labeled cells, upper left) using the FL1 channel. The data from the dot plot and the histogram are displayed in a separate table for convenience. The data in this table show gating subsets of both NC and NC FAM together with percent population not containing (FL1-H-) and containing NC FAM (FL1-H+). FSC and SSC represent size and cellular complexity (granularity), whereas FL1 is a measure of emitted fluorescence by using the FL1 (530/30) channel through excitation with the argon ion laser at 488 nm (530/30 denotes that the FL1 channel has a optical/bandpass filter centered at 530 nm with a width of 30 nm). Emission and excitation maximum of FAM is centered to 518 and 494 nm, respectively.

6.2 Biotin labeled miRNA mimics are biologically active in neuroblastoma cells

To investigate whether or not the addition of 3′-biotin to the miRNA mimics had any effect on its targeting, it was compared to that of unlabeled miRNA mimics in a luciferase based

approach. The MRE of each miRNA mimic was cloned into its respective reporter. Upon binding of the miRNA, expression of the luciferase protein that is encoded on the reporter will be repressed as a result of translational inhibition. Relative luciferase units (RLU) are measured using a luminometer and is used as means to detect binding of miRNA to its MRE. To account for factors such as transfection variability, pipetting inconsistencies, cell plating and toxicities, the Renilla luciferase was used to normalize the data. The Renilla luciferase does not contain any MREs and correlates to the amount of DNA transfected into the cells and the general ability to express protein as it encodes the constitutive CMV promoter (gives low to medium reporter expression). For testing whether the biological functions of the biotinylated mimics were intact or not, neuroblastoma cells were co-transfected with biotinylated mimics (bi-*mir-34a* and bi-*mir-21*) and the corresponding miRNA target luciferase reporter. As can be seen from Figure 6, a 50 and 20 % decrease in RLU was seen for bi-*mir-21* and *pre-mir-21* in targeting the 21-antisense MRE, respectively. In the case of *mir-34a*, roughly 30 % decrease in RLU could be observed for the biotinylated mimic by comparison to the negative control in aspects of targeting the *MYCN* 3'UTR. The non-biotinylated *mir-34a* was found not to be functional in targeting the same MRE. Here, a slight increase in RLU was observed (Figure 6B). Taken together, these results reveal that the biological function of both biotinylated mimics are intact and that they are suitable for use in the following pull-down study.

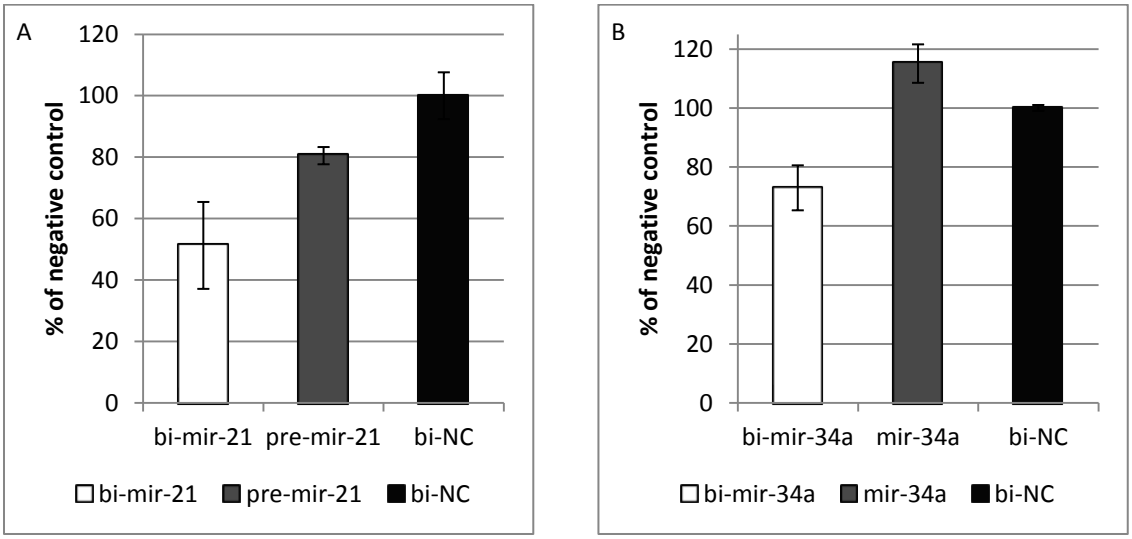

Figure 6 | Biotinylated mimics are functionally active in miRNA-mediated silencing. The biotinylated mimic of *mir-21* (A) and *mir-34a* (B) shows lower expression of relative luciferase units compared to the negative

control (bi-NC). For each microRNA, an additional mimic without biotin was tested to see whether the 21-antisense luciferase reporter (A) or the *MYCN* 3' UTR reporter (B) showed similar results. Data and standard deviance represents values from two independent experiments performed in SK-N-AS cells expressing intermediate endogenous levels of *mir-21* and low levels of *mir-34a*. In addition, the selectivity of the method was also undermined by the fact that the biotinylated, negative control did not enrich for their respective luciferase reporter targets. Data represents calculation of qPCR CT values by using the percent input method.

6.3 Successful enrichment of luciferase reporters approve the applicability of the method

To demonstrate the applicability of the mimic pull-down method, the same luciferase reporter constructs used in the luciferase assay was used as a control to test for the enrichment of *mir-21* and *mir-34a*. As demonstrated in Figure 7, both mimics show a high degree of enrichment of the luciferase transcript as opposed to the negative control *HPRT1* (a housekeeping gene).

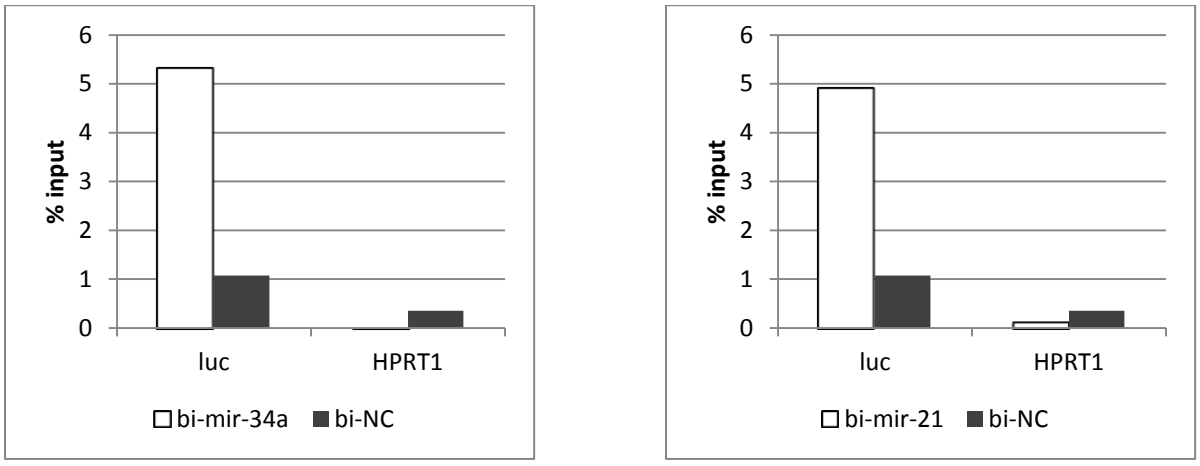

Figure 7 | Enrichment of luciferase reporters for *mir-21* and *mir-34a*. Both luciferase reporters which exhibited successful translational repression in the luciferase assay, was also shown to be enriched by bi-*mir-34a* and bi-*mir-21*. The pull-down showed selected affinity as HPRT1, a housekeeping gene, was not targeted by either miRNAs.

6.4 *mir-34a* targets *CCND1* and *MYCN* mRNAs in neuroblastoma cell line SK-N-BE(2)c

Isolation of mRNA bound to biotinylated miRNA mimics by using streptavidin-coated beads was employed to identify direct targets of *mir-34a*. Control samples were transfected with biotinylated *cel-mir-67* (bi-NC). As previously shown, biotinylation did not interfere with miRNA-mediated silencing (Figure 6). To ensure that the pull-down was specific, *HPRT1* (a housekeeping gene), was used as a control target. Neither the biotinylated mimics *mir-34a* or *mir-21*, nor the biotinylated negative control mimic (bi-NC) enriched for the control target *HPRT1*as shown in Figure 8A. Further, *CCND1* and *MYCN* were shown as targets by *mir-34a*. *SIRT1* is probably also a target of *mir-34a,* but it was not as clear as with *CCND1* and *MYCN*. We also tested several other targets in BE(2)c that have previously been described in the literature, but these were found not to be present in the pull-down. This include *DAAM1*, *HuR/ELAVL1*, *MAP3K9*, *PDCD4*, *E2F3* and *CDK6*. It should be noted that an arbitrary cut-off was set at 1 % relative to the input.

6.5 *MYCN* mRNA decrease upon *mir-34a* over-expression

To investigate whether the mRNAs that associate with *mir-34a* was affected by *mir-34a* over-expression, mRNAs were measured in BE(2)c transfected with bi-*mir-34a* and bi-NC (bi-*mir-cel-67*). Two non-biotinylated mimics, *mir-34a* and a negative control mimic (*cel-mir-67*), was also applied in the study for comparing the amount of altered gene expression. However, the non-biotinylated *mir-34a* mimic have previously been shown to not target the *MYCN* 3' UTR (Figure 6B) and it was additionally found to be unable in reducing the levels of *MYCN* after *mir-34a* over-expression (Figure 8D). Therefore, analysis of genes regulated by *mir-34a* may not be trustworthy. More importantly, over-expressing bi-*mir-34a* displays a 4-fold decrease in *MYCN* mRNA levels (Figure 8B) and 20 % increase of *CCND1* (Figure 8C). Additionally, two neuronal differentiation markers, *NPY* and *GAP43*, increased with 1.75 and 7.8 fold upon *mir-34a* over-expression, respectively (Figure 8C). This is consistent with the tumor suppressing role of *mir-34a* and targeting of *MYCN and CCND1*, two important members in accelerating tumor growth. Over-expression of *mir-34a* reveal 50 % reduction in *CDK6* levels, a positive regulator of the cell cycle, compared to the negative control. Another cyclin dependent kinase, *CDK4* was shown to be absent in BE(2)c

indicating that this neuroblastoma cell line relies on other CDKs such as *CDK6* to surpass the restriction point in the G_1 phase. Due to the absence of *CDK4* in the gene expression profiling it was not tested in the pull-down assay. *SIRT1*, a validated target of *mir-34a* in HCT116 human colon carcinoma cells[102] (Figure 8A), was not affected by *mir-34a* over-expression (Figure 8B). *HuR* was included as an arbitrary gene that has not shown to be a target of *mir-34a*. *HuR* displayed a ~1.5 fold increase upon *mir-34a* over-expression.

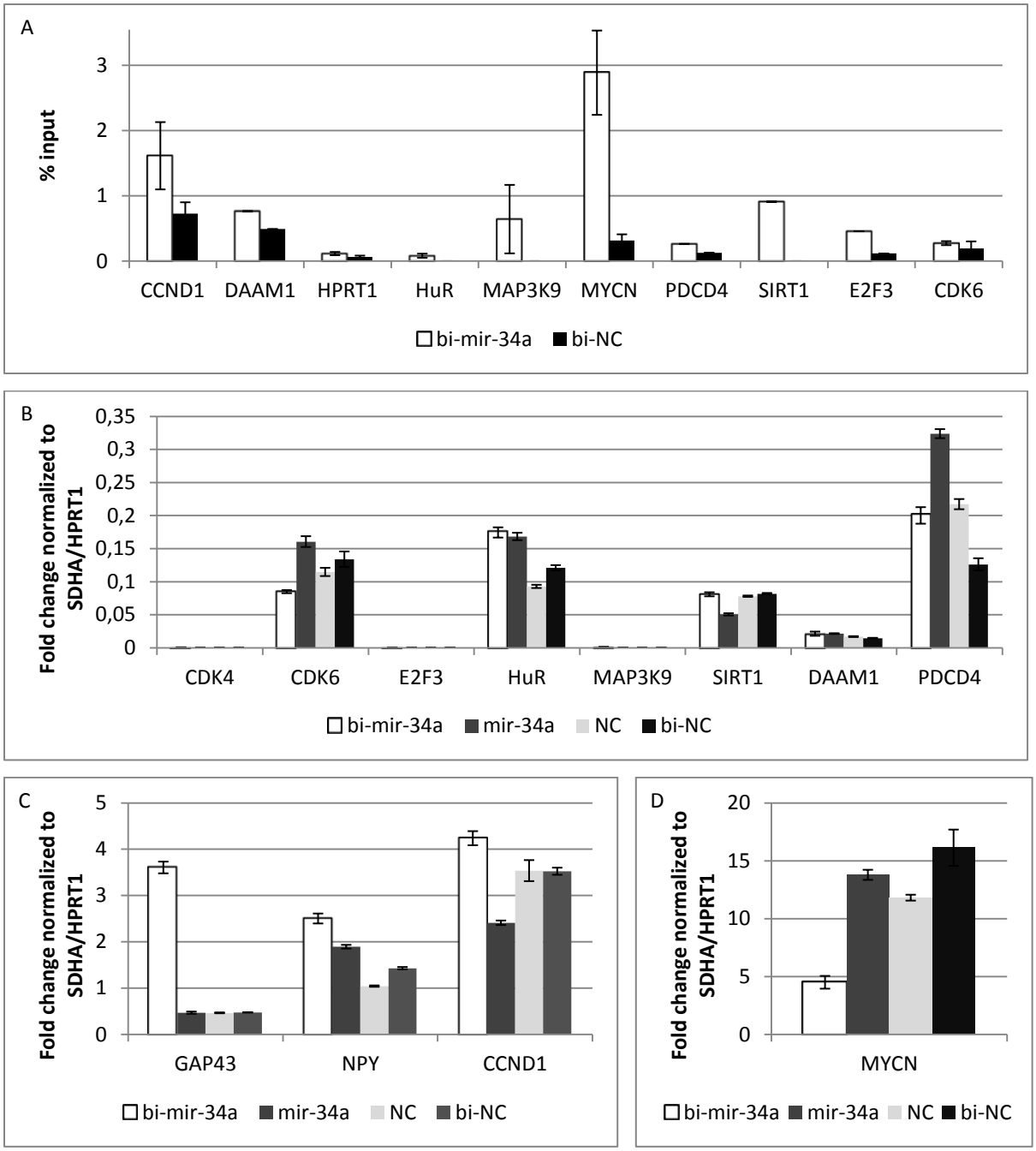

Figure 8 | Associated *mir-34a* targets *MYCN*, and not *CCND1*, correlate to down-regulated mRNA abundance after *mir-34a* over-expression and shows an increase in markers for neuronal differentiation. (A) Affinity purification of biotin tagged miRNA mimics by streptavidin enriches for targets *CCND1* and *MYCN* in BE(2)c. *HuR*, which is not a direct target of *mir-34a* but associates with *SIRT1*, is included as an arbitrary target and was shown to not be targeted by *mir-34a*. (B) *MYCN* levels reduced after *mir-34a* over-expression compared to negative control and are consistent with pull-down results as well as the luciferase study. (D) *CCND1* levels increased by 20 % compared to the negative control after *mir-34a* over-expression. Levels of the differentiation marker *NPY* and *GAP43* increased 1.75 and 7.8 fold as compared to the negative control.
All qPCR data were performed in duplicates from two independent experiments and normalized to two reference genes (*HPRT1* and *SDHA*) using the $2^{-\Delta CT}$ method of. Expression levels of SDHA/HPRT1 is set to 1 (SD<0.02).

6.6 The function of *mir-21* remains elusive in neuroblastoma

Isolation of mRNA bound to biotinylated miRNA mimics by using streptavidin-coated beads was employed to identify direct targets of *mir-21*. Control samples were transfected with biotinylated *cel-mir-67* (bi-NC). As previously shown, biotinylation did not interfere with miRNA-mediated silencing (Figure 6). To ensure that the pull-down was specific, *HPRT1* (a housekeeping gene), was used as a control target. Neither the biotinylated mimic nor the negative control enriched for the control target as shown in Figure 9A.

Of the previous reported targets of *mir-21*, none of these were detected in the pull-down. Interestingly, both *mir-21* and *pre-mir-21* increased the expression of the neuronal differentiation marker *GAP43* by more than 4-fold whereas *NPY* was reduced by 50 %. Moreover, there was a 4.3 fold reduction in *PDCD4* after over-expression of *pre-mir-21* compared to negative control (NC). *TGFβRII* and *FasL* was shown to be absent in BE(2)c. Not surprisingly, *TGFβRII* was not present in the pull-down. Due to the absent expression of FasL, it was not tested in the pull-down. *PTEN* levels were unchanged after over-expression of bi-*mir-21* and *pre-mir-21* (Figure 9B). *CDK6* expression levels decreased with 37 % upon over-expression of *pre-mir-21*.

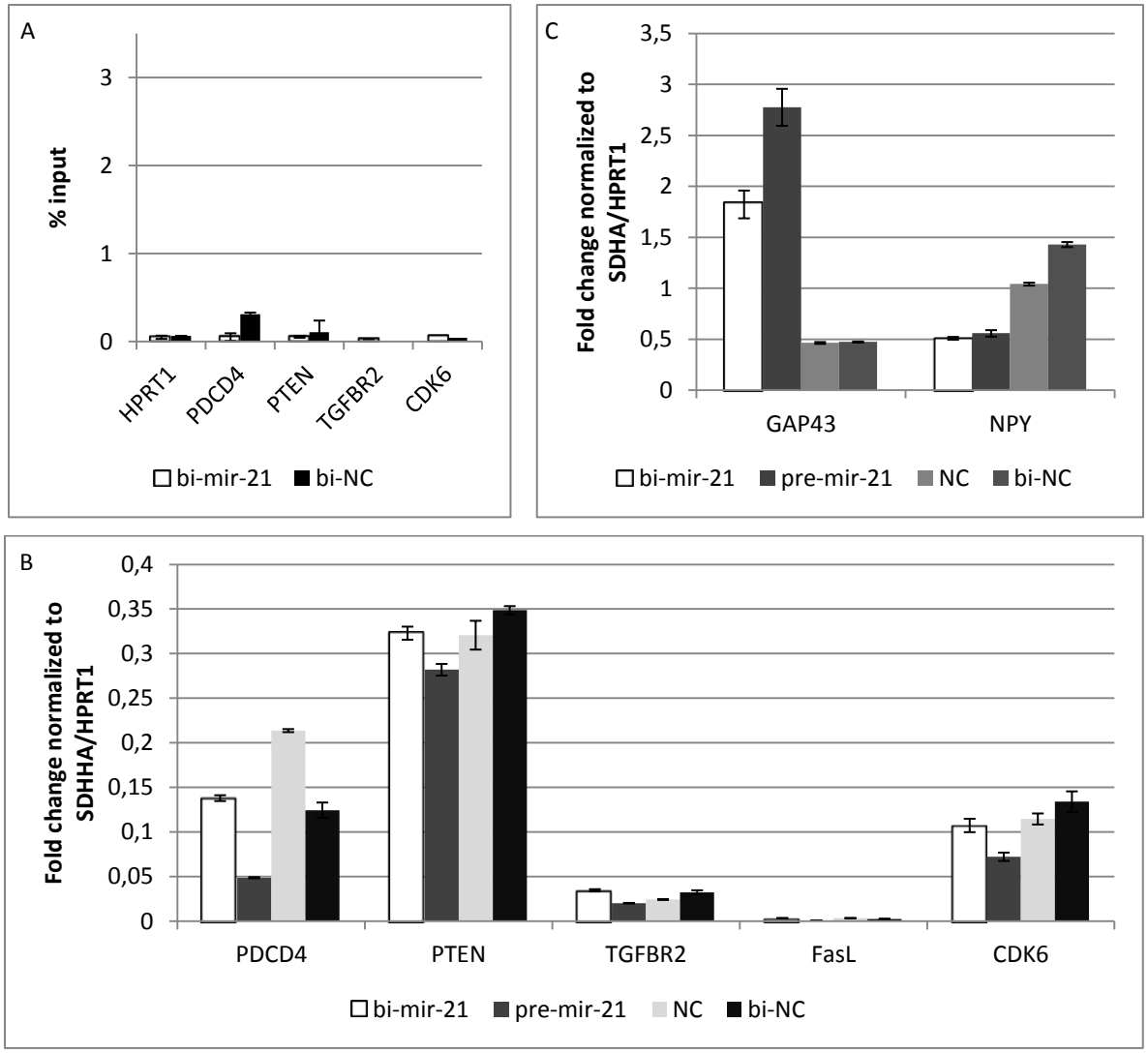

Figure 9 | The function of the tumor suppressor *mir-21* in neuroblastoma is yet unclear as it do not associate with targets cited in the literature. (A) Selected targets were not enriched in the pull-down of *mir-21*. (B) *mir-21* over-expression does not display a significant change in the associated targets. The neuronal differentiation marker GAP43 increased by more than 4-fold, whereas NPY showed a 50 % reduction.
All qPCR data were performed in duplicates from two independent experiments and normalized to two reference genes (*HPRT1* and *SDHA*) using the $2^{-\Delta CT}$ method of. Expression levels of SDHA/HPRT1 is set to 1 (SD<0.02).

7 Discussion

This thesis aims at addressing three important questions in the biology of cancer, and especially in regards to neuroblastoma. The first aim addressed the question of how to produce an in-house, simple, direct, reliable and cost-effective method for finding microRNA-mRNA targets that are associated with cancer (or any other disease for that matter). Secondly, the thesis aimed at understanding the role of the important tumor suppressor *mir-34a* in neuroblastoma. Third and last aim addressed the molecular biology of *mir-21*. Our research group has previously shown that *mir-21* reverse correlate strongly with *MYCN* expression, and has been seen as the strongest upregulated miRNA after *MYCN*-knockdown induced neuronal differentiation of SK-N-BE(2)c[89]. However, despite this fact no targets were identified for *mir-21*. In the following sections, the aims of this thesis are discussed in detail.

7.1 The biotin-labeled pull-down approach is a reliable method for exploring miRNA targets

The first aim of this thesis stresses the need for a method that could reliably detect miRNA targets in a fast, simple and cost-effective manner. Here, synthetic miRNA mimics was designed with a 3' end-labeled biotin tag that was affinity purified using streptavidin-coated magnetic beads. The captured mRNA was isolated and analyzed by qPCR. The biological function of the synthetic mimics (bi-*mir-21* and bi-*mir-34a*) were shown to be intact by (1) confirmed repression using a luciferase based approach, (2) enrichment of the luciferase reporters with *mir-21* and *mir-34a* and not with the biotinylated negative control mimic, and (3) known targets of *mir-34a*, *MYCN* and *CCND1*, was affinity purified using the biotin-labeled pull-down method. Results from the method can be collected in less than a week, and several hundreds to thousands of targets can be identified using this method by micro array analysis or high-throughput RNA sequencing (RNA-Seq). As a result of the conclusive data shown in this thesis, a micro array analysis will be completed as soon as possible to discover direct targets of both *mir-21* and *mir-34a* in neuroblastoma.

7.2 *MYCN* and *CCND1* are direct targets of *mir-34a* in neuroblastoma

As part of the second aim in this thesis, the method developed was used to search for direct targets of *mir-34a*. Induced differentiation of SK-N-BE together with increased expression of *mir-34a* has previously shed light on *mir-34a* as an important tumor suppressor in neuroblastoma. This was supported by the targeting of *mir-34a* to *CCND1* and *MYCN*, two important factors in driving cellular proliferation. *CCND1* mRNA was shown to be a direct target of *mir-34a* by the capture of streptavidin-coated beads. Additionally, *mir-34a* over-expression did not reduce endogenous levels of *CCND1* which would be expected by translational repression by *mir-34a*. A probable explanation for the un-changed levels of *CCND1* can also be correlated to a prolonged half-life. As the *CCND1* promoter is bound by the E-box of the N-myc oncoprotein, the data suggesting translational repression by *mir-34a* can be utterly convincing by measuring protein levels of cyclin D1 after *mir-34a* over-expression in MYCN non-amplified neuroblastoma cell lines (over-expression in *MYCN* amplified cells would give misleading results as a reduction would reflect reduced cyclin D1 by low *MYCN*-bound *CCND1*-promoter activity). Moreover, the half-life of *CCND1* has been shown to increase from 30 minutes in normal tissue to as much as three hours in human tumors[111]. Therefore, an increased mRNA abundance may be a result of prolonged mRNA half-life. The sequence of *CCND1* should therefore be explored to see whether it contains truncated regions or SNPs that can influence its half-life in SK-N-BE(2)c. It is possible that *CCND1* are directed to P-bodies.

In context to *MYCN*, capture of *mir-34a* identified *MYCN* as a direct target and was extensively down-regulated after over-expression of *mir-34a*. It was also shown that *mir-34a* targets the 3' UTR of *MYCN* in a luciferase based approach. The targeting of *MYCN* was consistent with the literature and increased the reliability of the method[98].

It has previously been shown that the *N-myc* oncoprotein positively regulates cyclin D1 by binding to the upstream promoter region. Therefore, over-expression of *mir-34a* can result in a synergistic down-regulation by direct and indirect targeting of cyclin D1 through *MYCN*. Taken together, loss of *mir-34a* and its suppressing function on *CCND1* and *MYCN* presents neuroblastoma tumors with G1/S progression and tumor growth. Moreover, this

thesis presents the scientific community with a novel inhibition of *CCND1* in neuroblastoma.

7.3 The neuroblastoma cell line SK-N-BE(2)c utilizes *CDK6* rather than *CDK4* to gain entry into the G1/S phase

Gene expression profiling of BE(2)c uncovered absence of *CDK4* in the neuroblastoma cell line BE(2)c. On the other hand, *mir-34a* over-expression reduced *CDK6* expression by 50 %. It is therefore likely that this neuroblastoma cell line relies on progression through G1/S by inactivating pRB through the concerted effects of *CDK6* and cyclin D1 (rather than *CDK4*). Previous studies have shown that a single mutation in *CDK6* can render it insensitive to $p16^{INK4a}$ (inactivates *CDK6* by binding to the ATP-binding site)[112]. It is therefore not unlikely that BE(2)c harbors the same mutation. Downstream effectors of cyclin dependent kinases are the "activator E2Fs" (E2F1-3) which have acquired their nickname due to their ability to activate gene expression of genes responsible to boost progression through the cell cycle clock (as opposed to E2F4-8 known as "repressor E2Fs"). These activators of cell cycle progression have collectively been shown to bind to the *MYCN* promoter in neuroblastoma[113]. Due to the absence of E2F3, E2F1 and/or E2F2 must therefore be believed to work in a synergistic fashion with *MYCN* to progress through the G1/S phase by the activation of the upstream activator, *CDK6*. Expression levels of E2F1 and E2F2 have not been described in SK-N-BE(2)c.

7.4 *SIRT1* is a possible, direct target in neuroblastoma and HuR is upregulated during *mir-34a* over-expression

SIRT1 was shown to be a probable target of *mir-34a* in neuroblastoma as it lay on the boundary of the 1 % cut-off. *mir-34a* has been shown to target *SIRT1* in the human colon carcinoma cell line HCT116 by reducing and elevating the levels of *SIRT1* by *mir-34a* over-expression and antisense *mir-34a*, respectively[102]. The same group also showed that *mir-34a* is capable of reducing *SIRT1* levels by targeting the 3' untranslated region. SIRT1 inhibits p21, a downstream target of p53 and a negative regulator of the cyclinD1-*CDK6* complex[102]. As such, *mir-34a* can down-regulate the levels of this complex at several levels (Figure 10). This thesis also showed that SIRT1levels were unchanged after *mir-34a* over-expression indicating translational repression. The absence of p21 in SK-N-BE(2)c[114] can be

an effect of absent *mir-34a* expression and thus alleviated SIRT1 inhibition (as well as mutated p53).

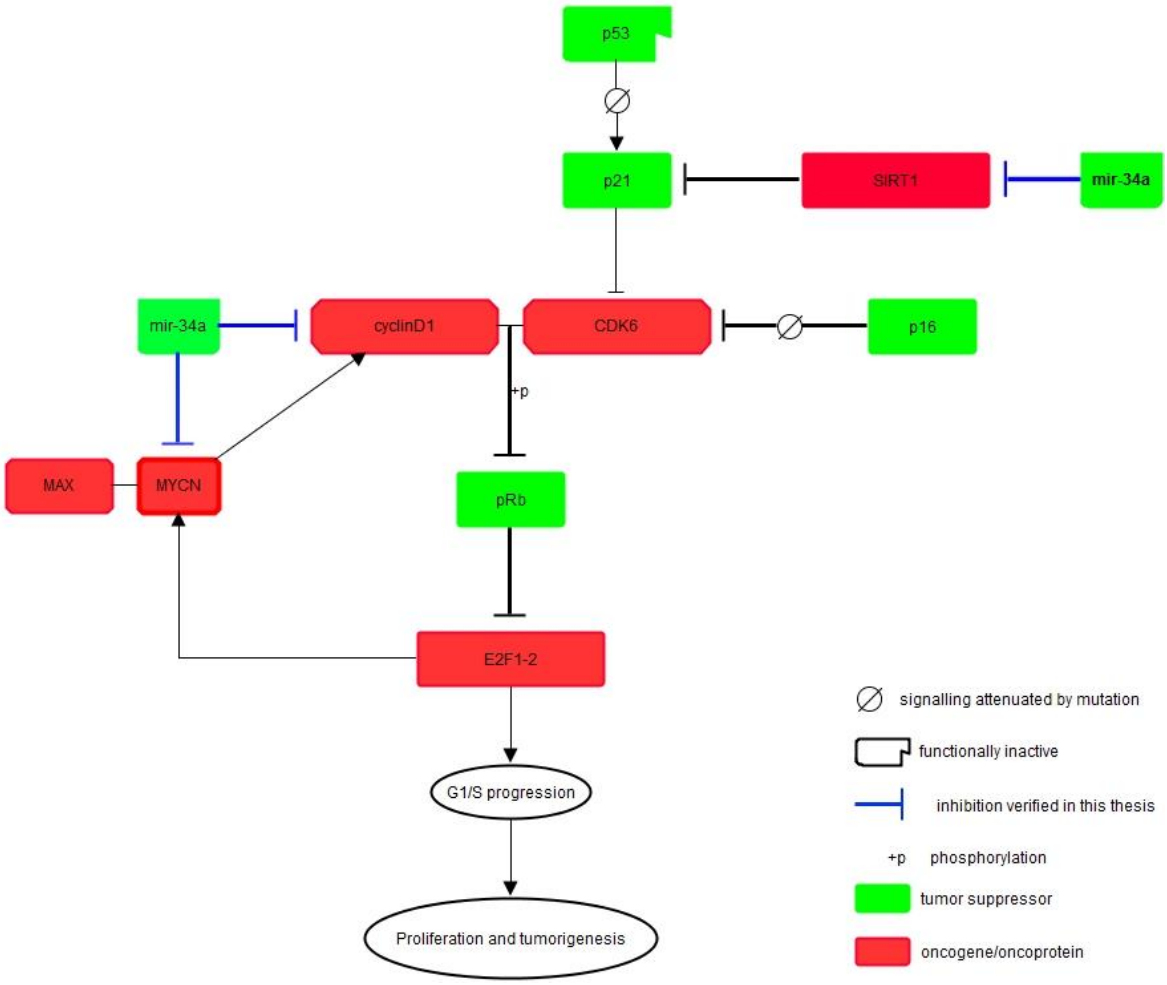

Figure 10 | mir-34a regulates the cell cycle complex cyclin D1-*CDK6* at multiple levels in the neuroblastoma cell line SK-N-BE(2)c. Inhibition of cyclin D1 can be achieved by the concerted effects of *mir-34a* suppression through both *MYCN* and *CCND1*. The absent p21 expression in BE(2)c is a possible effect of the mutated p53 variant and the loss of *mir-34a*. The loss of p21 elevates levels of *CDK6* and thus increases transcription of E2F1-2 by inhibiting the retinoblastoma protein. Down-regulation of *MYCN* by *mir-34a* is also strongly repressed by the feedback mechanism of E2F1-2. *CDK6* have been shown to harbor a single mutation that renders it inactive to $p16^{INK4a}$. Overall, *mir-34a* is a strong tumor suppressor in neuroblastoma.
The signaling pathway was designed using VANTED (Visualization and Analysis of Networks containing Experimental Data).

Hu-antigen R (HuR or *ELAVL1*), a family of RNA-binding proteins that selectively bind AU-rich elements (AREs) found in the 3' UTR (thus regulating gene expression by stabilizing mRNAs from selective degradation), is found to be overexpressed in a variety of cancers[115]. Surprisingly, *mir-34a* over-expression leads to a ~1.5 fold increase in *HuR*. Another group showed that HuR recruits *let-7*-loaded RISC to the Myc 3' UTR by binding to a proximal region of the *let-7* MRE[116]. In context to this study, our group has previously shown that *let-7c, let-7f* and *let-7d* increase 1.7-2.6 fold upon *MYCN*-knockdown induced differentiation of BE(2)c[89]. m*ir-34a* targets *MYCN* both directly and indirectly, and therefore a similar scenario would apply here. It is consequently likely that HuR up-regulation is a result of HuR aiding in the differentiation by enhancing *let-7* miRNA-mediated silencing.

7.5 The role of mir-21 in neuroblastoma remains elusive

BE(2)c encompasses very low levels of *mir-21*. This may be due to mutated version of p53 which is unable to bind to the *mir-21* promoter. The *mir-21* promoter is known to contain an *AP-1* binding site[88]. Data from our lab show that *AP-1* is negatively regulated by *MYCN* in neuroblastoma (unpublished data). Therefore it comes as no surprise that we have previously reported that there are low levels of *mir-21* in BE(2)c. Our lab has previously shown *mir-21* as the microRNA that is highest expressed after *MYCN*-knockdown induced neuronal differentiation of BE(2)c[89] . *PTEN* and *PDCD4* have been validated targets by *mir-21* in other cancers[117, 118]. The results of this thesis showed that neither *PTEN* nor *PDCD4* changed after over-expression of *mir-21*. However, there were conflicting results using the biotinylated *mir-21* versus *pre-mir-21* in context to regulation of *PDCD4* where *pre-mir-21* down-regulated *PDCD4* by more than 60 %. This result might be explained by off-target effects specific for *pre-mir-21*. More imperative results showed that *PTEN* and *PDCD4* protein levels were not reduced after *pre-mir-21* over-expression[89]. Taken together, *PDCD4* and *PTEN* are not targets of *mir-21* in the neuroblastoma cell line BE(2)c.

None of the other targets tested in the pull-down were enriched. This includes *TGFβRII* and *CDK6*. Endogenous *CDK6* have previously been shown to not be targeted by the introduction of anti-sense *mir-21* in MCF-7 breast cancer cell lines (luciferase and western

blotting) [83]. The changes of *CDK6* expression levels as a result of *mir-21* over-expression are more likely to be an effect of *mir-21* induced differentiation rather than direct association.

Treatment with *pre-mir-21* or bi-*mir-21* did not induce neurite outgrowth (data not shown). This is consistent with the lack of the early neuronal differentiation marker neuropeptide Y (*NPY*). Surprisingly, *GAP43* expression (another neuronal differentiation marker) increased 4-fold as opposed to the 50 % reduction of *NPY*. Despite the fact that *mir-21* cannot induce differentiation of neuroblastoma cells, these data might indicate that *mir-21* is involved in the early processes of neurite sprouting by inducing GAP-43 expression.

mir-21 has been shown to be involved in neuroblastoma drug resistance, by direct effect on the sensitivity to cisplatin in neuroblastoma cell lines[119]. Here, they show that over-expression of *pre-mir-21* increased the resistance to cisplatin treatment in neuroblastoma cells SH-SY-5Y and SK-N-BE(2)-M17. However, *mir-21* expression can both be up and down-regulated after chemotherapy as shown by SOLiD sequencing (Supplementary table 1) and as such the role of *mir-21* related to drug resistance in neuroblastoma is therefore unclear. The same group also shows that *PTEN* mRNA and protein levels are reduced by cisplatin-treatment (infers 3.7-fold *mir-21* up-regulation) and ectopic over-expression of *pre-mir-21* in SH-SY-5Y neuroblastoma cells, respectively. It could therefore be interesting to see whether the biotinylated *mir-21* captures *PTEN* mRNA in SH-SY-5Y neuroblastoma cell lines.

7.6 Causes for inconsistent experimental data

There were some inconsistencies in the luciferase experiment. This is explained here. To test if the attachment of biotin to the mimic had any impact on the targeting effect, an unbiotinylated mimic for each microRNA was tested. Here, the biotinylated *mir-21* showed considerable lower expression of RLU than *pre-mir-21*. This could come from the fact that the hairpin of *pre-mir-21* needs to be cleaved off by Drosha and its co-factor DGCR8 before the mimic is able to be loaded to the RISC. This means that bi-*mir-21*, unlike *pre-mir-21*, can circumvent the nucleus before being able to find its target. It is therefore most likely that this is the reason for *pre-mir-21* showing a lesser degree of RLU knockdown in the

luciferase assays. In the case of *mir-34a*, the biotinylated mimic showed a reasonable amount of knockdown whereas the unbiotinylated mimic did not. Further analysis revealed that the passenger strand of *mir-34a* was completely complementary to the guide strand. Under normal, biological conditions each miRNA duplex are not 100 % complementary to each other – they are known to contain mismatches and bulges at different positions which may aid in the unwinding of the strands from each other. Duplexes lacking this complementarity may not dissociate from each other, as may be the case here, therefore they will not find their targets and thus would not be functional. Therefore it is vital that when designing miRNA mimics, mismatches and bulges are taken into the equation.

7.7 Further experiments

As microRNAs have the potential to act as pluripotent regulators of gene expression this method is invariably a reliable method to detect the many binding partners microRNAs can have in cells. Our lab will conduct further investigations of the role of *mir-21* and *mir-34a* in neuroblastoma by the aid of micro-array analysis. We have already been in contact with the micro-array core facility, and the experiment will be performed during the summer. So far, no targets were validated for *mir-21* and understanding its role would therefore be of great clinical interest as this miRNA is found dysregulated in many types of human cancers. The use of micro-array will most likely reveal targets of *mir-21* in neuroblastoma. These targets can be validated by the same approaches used in this thesis. Moreover, *MYCN*, *CCND1* and *SIRT1* were shown to be targets of *mir-34a* (the latter less convincing). These targets will be further tested by a luciferase based approach as well as western blotting.

Western blotting to detect Ago2 was performed on pull-down and input samples from BE(2)c (data not shown). The underlying reason was to show that biotinylated miRNAs find their way to the RISC-Ago2 complex and are thus functionally active. However, the western blot did only show Ago2 protein in the input samples whereas the pull-down however did not. A reason for this could be that only 5 % pull-down sample was applied for detecting

Ago2. Western blotting of Ago2 will therefore be performed on the pull-down of *mir-21* and *mir-34a* in the near future (by using the entire pull-down for western).

8 Conclusion

With epigenetic silencing of *mir-34a,* or LOH 1p36, the cell loses its capability to suppress the oncogenic function of two important oncoproteins, cyclin D1 and N-myc. Another target *SIRT1*, albeit not as dominant in the pull-down, is also a target of *mir-34a*. As such, attenuated *mir-34a* expression can in part explain the tumorigenesis of neuroblastoma.

Over-expression of *mir-34a* and *mir-21* lead to an increase in neuronal differentiation. The thesis did not present any new targets in regards to *mir-21* by using the neuroblastoma SK-N-BE(2)c cell line.

Collectively, *mir-21* and *mir-34a* may prove to have potential as targets in the treatment of high-risk neuroblastomas.

9 Appendix

Supplementary table 1:

Expression profile of *mir-21* and *mir-34a* in various neuroblastoma cell lines.

Supplementary table 2:

List of qPCR primers.

Supplementary table 1 | Expression of *mir-21*-5p (UAGCUUAUCAGACUGAUGUUGA) and *mir-34-5p* (UGGCAGUGUCUUAGCUGGUUGU) in various neuroblastoma cell lines. Numbers represent mean transcripts found by SOLiD sequencing. For further information about these data, please contact the author.

	21-5p	34-5p
SKNBE(1)	3128,7	90,1
SKNBE(2)c	699,0	19,4
SMS KAN	133,7	2615,3
SMS KANR	1308,5	56,5
SMS KCN	140954,0	2661,2
SMS KCNR	699,0	19,4
CHLA-12	97,7	2089,3
CHLA-13	555,6	564,0
CHLA-15	571,4	1367,0
CHLA-20	1523,4	208,9
NBL W	40,8	4199,5
NBL WR	69,5	1002,3

Supplementary table 2 | List of qPCR primers used in this thesis.

Primer	Forward (5′-3′)	Reverse (5′-3′)
CCND1	CCGTCCATGCGGAAGATC	ATGGCCAGCGGGAAGAC
CDK4	CTGTGGAAACTCTGAAGCCGA	TGAGATGGAGGAGTCGGGAG
CDK6	GACTGGCCTAGAGATGTTGCC	GTATGGGTGAGACAGGGCAC
DAAM1	AGGTGGCGGACCTCACAGCA	TCCAGGCGAGGGTCCACCTG
E2F3	GCAGCCTCCTCTACACCAC	AGGTACTGATGACCGCTTTCT
FasL	CTGAAGAAGAGAGGGAACCACA	AGCTCCTTCTGTAGGTGGAAGA
HuR/ELAVL1	TCTCACTTGTAAGTCACCGCCAGTA	GCAAGTCACTGTAAACGGAACATCA
HPRT1	TGACACTGGCAAAACAATGCA	GGTCCTTTTCACCAGCAAGCT
luciferase	ATGAACGTGAATTGCTCAACAG	TAAAACCGGGAGGTAGATGAGA
MAP3K9	GTGCCCATCGACATTGAAGA	TCCACGAGGGAATGGGATAC
MYCN	CGACCACAAGGCCCTCAGTA	TGGTGTTGGAGGAGGAACGC
PTEN	TGCAGAGTTGCACAATATCCTT	GTCATCTTCACTTAGCCATTGGT
PDCD4	ATGAGCACAACTGATGTGGAAA	ACAGCTCTAGCAATAAACTGGC
SPRY2	GGCTTTCAGAACTATGAGCCAAAT	ATTTGGCTCATAGTTCTGAAAGCC
TGFBR2	GTAGCTCTGATGAGTGCAATGAC	CAGATATGGCAACTCCCAGTG

10 References

1. Brodeur, G.M. Neuroblastoma: biological insights into a clinical enigma. *Nature reviews. Cancer* **3**, 203-216 (2003).
2. Maris, J.M., Hogarty, M.D., Bagatell, R. & Cohn, S.L. Neuroblastoma. *Lancet* **369**, 2106-2120 (2007).
3. Kaatsch, P. Epidemiology of childhood cancer. *Cancer treatment reviews* **36**, 277-285 (2010).
4. Brodeur, G.M. et al. International criteria for diagnosis, staging, and response to treatment in patients with neuroblastoma. *Journal of clinical oncology : official journal of the American Society of Clinical Oncology* **6**, 1874-1881 (1988).
5. Brodeur, G.M. et al. Revisions of the international criteria for neuroblastoma diagnosis, staging, and response to treatment. *Journal of clinical oncology : official journal of the American Society of Clinical Oncology* **11**, 1466-1477 (1993).
6. Eklof, O., Sandstedt, B., Thonell, S. & Ahstrom, L. Spontaneous regression of stage IV neuroblastoma. *Acta paediatrica Scandinavica* **72**, 473-476 (1983).
7. Tonini, G.P. et al. MYCN oncogene amplification in neuroblastoma is associated with worse prognosis, except in stage 4s: the Italian experience with 295 children. *Journal of clinical oncology : official journal of the American Society of Clinical Oncology* **15**, 85-93 (1997).
8. Mullassery, D., Dominici, C., Jesudason, E.C., McDowell, H.P. & Losty, P.D. Neuroblastoma: contemporary management. *Archives of disease in childhood. Education and practice edition* **94**, 177-185 (2009).
9. Modak, S. Updates in the treatment of neuroblastoma. *Clinical advances in hematology & oncology : H&O* **9**, 74-76 (2011).
10. Modak, S. & Cheung, N.K. Neuroblastoma: Therapeutic strategies for a clinical enigma. *Cancer treatment reviews* **36**, 307-317 (2010).
11. Jiang, M., Stanke, J. & Lahti, J.M. in Current Topics in Developmental Biology, Vol. Volume 94. (ed. A.D. Michael) 77-127 (Academic Press, 2011).
12. Zimmerman, K.A. et al. Differential expression of myc family genes during murine development. *Nature* **319**, 780-783 (1986).
13. Deyell, R.J. & Attiyeh, E.F. Advances in the understanding of constitutional and somatic genomic alterations in neuroblastoma. *Cancer genetics* **204**, 113-121 (2011).
14. Noguchi, T. et al. Amplification of a DEAD box gene (DDX1) with the MYCN gene in neuroblastomas as a result of cosegregation of sequences flanking the MYCN locus. *Genes, chromosomes & cancer* **15**, 129-133 (1996).
15. Squire, J.A. et al. Co-amplification of MYCN and a DEAD box gene (DDX1) in primary neuroblastoma. *Oncogene* **10**, 1417-1422 (1995).
16. Amler, L.C., Schurmann, J. & Schwab, M. The DDX1 gene maps within 400 kbp 5' to MYCN and is frequently coamplified in human neuroblastoma. *Genes, chromosomes & cancer* **15**, 134-137 (1996).
17. Wimmer, K. et al. Co-amplification of a novel gene, NAG, with the N-myc gene in neuroblastoma. *Oncogene* **18**, 233-238 (1999).
18. Varshavsky, A. The N-end rule pathway of protein degradation. *Genes to cells : devoted to molecular & cellular mechanisms* **2**, 13-28 (1997).
19. Cohn, S.L. et al. Prolonged N-myc protein half-life in a neuroblastoma cell line lacking N-myc amplification. *Oncogene* **5**, 1821-1827 (1990).
20. Ayer, D.E., Kretzner, L. & Eisenman, R.N. Mad: a heterodimeric partner for Max that antagonizes Myc transcriptional activity. *Cell* **72**, 211-222 (1993).
21. Ayer, D.E. & Eisenman, R.N. A switch from Myc:Max to Mad:Max heterocomplexes accompanies monocyte/macrophage differentiation. *Genes & development* **7**, 2110-2119 (1993).

22. Hurlin, P.J. et al. Mad3 and Mad4: novel Max-interacting transcriptional repressors that suppress c-myc dependent transformation and are expressed during neural and epidermal differentiation. *The EMBO journal* **14**, 5646-5659 (1995).
23. Zervos, A.S., Gyuris, J. & Brent, R. Mxi1, a protein that specifically interacts with Max to bind Myc-Max recognition sites. *Cell* **72**, 223-232 (1993).
24. Hurlin, P.J., Queva, C. & Eisenman, R.N. Mnt, a novel Max-interacting protein is coexpressed with Myc in proliferating cells and mediates repression at Myc binding sites. *Genes & development* **11**, 44-58 (1997).
25. Bui, T.V. & Mendell, J.T. Myc: Maestro of MicroRNAs. *Genes & cancer* **1**, 568-575 (2010).
26. Morin, R.D. et al. Application of massively parallel sequencing to microRNA profiling and discovery in human embryonic stem cells. *Genome research* **18**, 610-621 (2008).
27. Kozomara, A. & Griffiths-Jones, S. miRBase: integrating microRNA annotation and deep-sequencing data. *Nucleic acids research* **39**, D152-157 (2011).
28. Griffiths-Jones, S., Saini, H.K., van Dongen, S. & Enright, A.J. miRBase: tools for microRNA genomics. *Nucleic acids research* **36**, D154-158 (2008).
29. Griffiths-Jones, S., Grocock, R.J., van Dongen, S., Bateman, A. & Enright, A.J. miRBase: microRNA sequences, targets and gene nomenclature. *Nucleic acids research* **34**, D140-144 (2006).
30. Griffiths-Jones, S. The microRNA Registry. *Nucleic acids research* **32**, D109-111 (2004).
31. miRBase.
32. Lytle, J.R., Yario, T.A. & Steitz, J.A. Target mRNAs are repressed as efficiently by microRNA-binding sites in the 5' UTR as in the 3' UTR. *Proceedings of the National Academy of Sciences of the United States of America* **104**, 9667-9672 (2007).
33. Kloosterman, W.P., Wienholds, E., Ketting, R.F. & Plasterk, R.H. Substrate requirements for let-7 function in the developing zebrafish embryo. *Nucleic Acids Res.* **32**, 6284-6291 (2004).
34. Rodriguez, A., Griffiths-Jones, S., Ashurst, J.L. & Bradley, A. Identification of mammalian microRNA host genes and transcription units. *Genome research* **14**, 1902-1910 (2004).
35. Scott, M.S., Avolio, F., Ono, M., Lamond, A.I. & Barton, G.J. Human miRNA precursors with box H/ACA snoRNA features. *PLoS Comput Biol* **5**, e1000507 (2009).
36. Kiss, T. Small nucleolar RNAs: an abundant group of noncoding RNAs with diverse cellular functions. *Cell* **109**, 145-148 (2002).
37. Bachellerie, J.P., Cavaille, J. & Huttenhofer, A. The expanding snoRNA world. *Biochimie* **84**, 775-790 (2002).
38. Winter, J., Jung, S., Keller, S., Gregory, R.I. & Diederichs, S. Many roads to maturity: microRNA biogenesis pathways and their regulation. *Nature cell biology* **11**, 228-234 (2009).
39. Kim, V.N., Han, J. & Siomi, M.C. Biogenesis of small RNAs in animals. *Nature reviews. Molecular cell biology* **10**, 126-139 (2009).
40. Siomi, H. & Siomi, M.C. On the road to reading the RNA-interference code. *Nature* **457**, 396-404 (2009).
41. Treiber, T., Treiber, N. & Meister, G. Regulation of microRNA biogenesis and function. *Thrombosis and haemostasis* **107**, 605-610 (2012).
42. Denli, A.M., Tops, B.B., Plasterk, R.H., Ketting, R.F. & Hannon, G.J. Processing of primary microRNAs by the Microprocessor complex. *Nature* **432**, 231-235 (2004).
43. Park, J.E. et al. Dicer recognizes the 5' end of RNA for efficient and accurate processing. *Nature* **475**, 201-205 (2011).
44. Pillai, R.S., Artus, C.G. & Filipowicz, W. Tethering of human Ago proteins to mRNA mimics the miRNA-mediated repression of protein synthesis. *RNA* **10**, 1518-1525 (2004).
45. Su, H., Trombly, M.I., Chen, J. & Wang, X. Essential and overlapping functions for mammalian Argonautes in microRNA silencing. *Genes & development* **23**, 304-317 (2009).

46. Filipowicz, W., Bhattacharyya, S.N. & Sonenberg, N. Mechanisms of post-transcriptional regulation by microRNAs: are the answers in sight? *Nature reviews. Genetics* **9**, 102-114 (2008).
47. Doench, J.G. & Sharp, P.A. Specificity of microRNA target selection in translational repression. *Genes & development* **18**, 504-511 (2004).
48. Brennecke, J., Stark, A., Russell, R.B. & Cohen, S.M. Principles of microRNA-target recognition. *PLoS biology* **3**, e85 (2005).
49. Lewis, B.P., Burge, C.B. & Bartel, D.P. Conserved seed pairing, often flanked by adenosines, indicates that thousands of human genes are microRNA targets. *Cell* **120**, 15-20 (2005).
50. Grimson, A. MicroRNA targeting specificity in mammals: determinants beyond seed pairing. *Mol. Cell* **27**, 91-105 (2007).
51. Nielsen, C.B. Determinants of targeting by endogenous and exogenous microRNAs and siRNAs. *RNA* **13**, 1894-1910 (2007).
52. Gaidatzis, D., van Nimwegen, E., Hausser, J. & Zavolan, M. Inference of miRNA targets using evolutionary conservation and pathway analysis. *BMC Bioinformatics* **8**, 69 (2007).
53. Grimson, A. et al. MicroRNA targeting specificity in mammals: determinants beyond seed pairing. *Molecular cell* **27**, 91-105 (2007).
54. Wu, L., Fan, J. & Belasco, J.G. MicroRNAs direct rapid deadenylation of mRNA. *Proceedings of the National Academy of Sciences of the United States of America* **103**, 4034-4039 (2006).
55. Behm-Ansmant, I. et al. mRNA degradation by miRNAs and GW182 requires both CCR4:NOT deadenylase and DCP1:DCP2 decapping complexes. *Genes & development* **20**, 1885-1898 (2006).
56. Nottrott, S., Simard, M.J. & Richter, J.D. Human let-7a miRNA blocks protein production on actively translating polyribosomes. *Nature structural & molecular biology* **13**, 1108-1114 (2006).
57. Pillai, R.S. et al. Inhibition of translational initiation by Let-7 MicroRNA in human cells. *Science* **309**, 1573-1576 (2005).
58. Humphreys, D.T., Westman, B.J., Martin, D.I. & Preiss, T. MicroRNAs control translation initiation by inhibiting eukaryotic initiation factor 4E/cap and poly(A) tail function. *Proceedings of the National Academy of Sciences of the United States of America* **102**, 16961-16966 (2005).
59. Chendrimada, T.P. et al. MicroRNA silencing through RISC recruitment of eIF6. *Nature* **447**, 823-828 (2007).
60. Petersen, C.P., Bordeleau, M.E., Pelletier, J. & Sharp, P.A. Short RNAs repress translation after initiation in mammalian cells. *Molecular cell* **21**, 533-542 (2006).
61. Hsu, R.J. & Tsai, H.J. Performing the Labeled microRNA pull-down (LAMP) assay system: an experimental approach for high-throughput identification of microRNA-target mRNAs. *Methods Mol Biol* **764**, 241-247 (2011).
62. Lal, A. et al. Capture of microRNA-bound mRNAs identifies the tumor suppressor miR-34a as a regulator of growth factor signaling. *PLoS genetics* **7**, e1002363 (2011).
63. Orom, U.A. & Lund, A.H. Isolation of microRNA targets using biotinylated synthetic microRNAs. *Methods* **43**, 162-165 (2007).
64. Thomson, D.W., Bracken, C.P. & Goodall, G.J. Experimental strategies for microRNA target identification. *Nucleic acids research* **39**, 6845-6853 (2011).
65. Chi, S.W., Zang, J.B., Mele, A. & Darnell, R.B. Argonaute HITS-CLIP decodes microRNA-mRNA interaction maps. *Nature* **460**, 479-486 (2009).
66. Hafner, M. et al. Transcriptome-wide identification of RNA-binding protein and microRNA target sites by PAR-CLIP. *Cell* **141**, 129-141 (2010).
67. Vatolin, S., Navaratne, K. & Weil, R.J. A novel method to detect functional microRNA targets. *Journal of molecular biology* **358**, 983-996 (2006).

68. Andachi, Y. A novel biochemical method to identify target genes of individual microRNAs: identification of a new Caenorhabditis elegans let-7 target. *RNA* **14**, 2440-2451 (2008).
69. Green, N.M. Avidin and streptavidin. *Methods in enzymology* **184**, 51-67 (1990).
70. Tong, X. & Smith, L.M. Solid-phase method for the purification of DNA sequencing reactions. *Analytical chemistry* **64**, 2672-2677 (1992).
71. Lee, Y. et al. MicroRNA genes are transcribed by RNA polymerase II. *The EMBO journal* **23**, 4051-4060 (2004).
72. Gilbert, F. et al. Human neuroblastomas and abnormalities of chromosomes 1 and 17. *Cancer research* **44**, 5444-5449 (1984).
73. Chan, J.A., Krichevsky, A.M. & Kosik, K.S. MicroRNA-21 is an antiapoptotic factor in human glioblastoma cells. *Cancer research* **65**, 6029-6033 (2005).
74. Qian, B. et al. High miR-21 expression in breast cancer associated with poor disease-free survival in early stage disease and high TGF-beta1. *Breast cancer research and treatment* **117**, 131-140 (2009).
75. Yan, L.X. et al. MicroRNA miR-21 overexpression in human breast cancer is associated with advanced clinical stage, lymph node metastasis and patient poor prognosis. *RNA* **14**, 2348-2360 (2008).
76. Gabriely, G. et al. MicroRNA 21 promotes glioma invasion by targeting matrix metalloproteinase regulators. *Molecular and cellular biology* **28**, 5369-5380 (2008).
77. Corsten, M.F. et al. MicroRNA-21 knockdown disrupts glioma growth in vivo and displays synergistic cytotoxicity with neural precursor cell delivered S-TRAIL in human gliomas. *Cancer research* **67**, 8994-9000 (2007).
78. Meng, F. et al. MicroRNA-21 regulates expression of the PTEN tumor suppressor gene in human hepatocellular cancer. *Gastroenterology* **133**, 647-658 (2007).
79. Selaru, F.M. et al. MicroRNA-21 is overexpressed in human cholangiocarcinoma and regulates programmed cell death 4 and tissue inhibitor of metalloproteinase 3. *Hepatology* **49**, 1595-1601 (2009).
80. Dillhoff, M., Liu, J., Frankel, W., Croce, C. & Bloomston, M. MicroRNA-21 is overexpressed in pancreatic cancer and a potential predictor of survival. *Journal of gastrointestinal surgery : official journal of the Society for Surgery of the Alimentary Tract* **12**, 2171-2176 (2008).
81. Lv, L. et al. MicroRNA-21 is overexpressed in renal cell carcinoma. *The International journal of biological markers*, 0 (2013).
82. Zhang, J.G. et al. MicroRNA-21 (miR-21) represses tumor suppressor PTEN and promotes growth and invasion in non-small cell lung cancer (NSCLC). *Clinica chimica acta; international journal of clinical chemistry* **411**, 846-852 (2010).
83. Frankel, L.B. et al. Programmed cell death 4 (PDCD4) is an important functional target of the microRNA miR-21 in breast cancer cells. *The Journal of biological chemistry* **283**, 1026-1033 (2008).
84. Wang, K. & Li, P.F. Foxo3a regulates apoptosis by negatively targeting miR-21. *The Journal of biological chemistry* **285**, 16958-16966 (2010).
85. Hatley, M.E. et al. Modulation of K-Ras-dependent lung tumorigenesis by MicroRNA-21. *Cancer cell* **18**, 282-293 (2010).
86. Sayed, D. et al. MicroRNA-21 targets Sprouty2 and promotes cellular outgrowths. *Molecular biology of the cell* **19**, 3272-3282 (2008).
87. Papagiannakopoulos, T., Shapiro, A. & Kosik, K.S. MicroRNA-21 targets a network of key tumor-suppressive pathways in glioblastoma cells. *Cancer research* **68**, 8164-8172 (2008).
88. Fujita, S. et al. miR-21 Gene expression triggered by AP-1 is sustained through a double-negative feedback mechanism. *Journal of molecular biology* **378**, 492-504 (2008).
89. Buechner, J. et al. Inhibition of mir-21, which is up-regulated during MYCN knockdown-mediated differentiation, does not prevent differentiation of neuroblastoma cells. *Differentiation; research in biological diversity* **81**, 25-34 (2011).

90. Attiyeh, E.F. et al. Chromosome 1p and 11q deletions and outcome in neuroblastoma. *The New England journal of medicine* **353**, 2243-2253 (2005).
91. White, P.S. et al. Definition and characterization of a region of 1p36.3 consistently deleted in neuroblastoma. *Oncogene* **24**, 2684-2694 (2005).
92. Guo, C. et al. Allelic deletion at 11q23 is common in MYCN single copy neuroblastomas. *Oncogene* **18**, 4948-4957 (1999).
93. Hashimoto, N. et al. Frequent deletions of material from chromosome arm 1p in oligodendroglial tumors revealed by double-target fluorescence in situ hybridization and microsatellite analysis. *Genes, chromosomes & cancer* **14**, 295-300 (1995).
94. Poetsch, M. et al. An increased frequency of numerical chromosomal abnormalities and 1p36 deletions in isolated cells from paraffin sections of malignant melanomas by means of interphase cytogenetics. *Cancer genetics and cytogenetics* **104**, 146-152 (1998).
95. Mori, N. et al. Chromosome band 1p36 contains a putative tumor suppressor gene important in the evolution of chronic myelocytic leukemia. *Blood* **92**, 3405-3409 (1998).
96. Bieche, I., Khodja, A. & Lidereau, R. Deletion mapping in breast tumor cell lines points to two distinct tumor-suppressor genes in the 1p32-pter region, one of deleted regions (1p36.2) being located within the consensus region of LOH in neuroblastoma. *Oncology reports* **5**, 267-272 (1998).
97. Cheung, T.H. et al. Clinicopathologic significance of loss of heterozygosity on chromosome 1 in cervical cancer. *Gynecologic oncology* **96**, 510-515 (2005).
98. Wei, J.S. et al. The MYCN oncogene is a direct target of miR-34a. *Oncogene* **27**, 5204-5213 (2008).
99. Brodeur, G.M., Seeger, R.C., Schwab, M., Varmus, H.E. & Bishop, J.M. Amplification of N-myc in untreated human neuroblastomas correlates with advanced disease stage. *Science* **224**, 1121-1124 (1984).
100. Sun, F. et al. Downregulation of CCND1 and CDK6 by miR-34a induces cell cycle arrest. *FEBS letters* **582**, 1564-1568 (2008).
101. Tivnan, A. et al. MicroRNA-34a is a potent tumor suppressor molecule in vivo in neuroblastoma. *BMC cancer* **11**, 33 (2011).
102. Yamakuchi, M., Ferlito, M. & Lowenstein, C.J. miR-34a repression of SIRT1 regulates apoptosis. *Proceedings of the National Academy of Sciences of the United States of America* **105**, 13421-13426 (2008).
103. Kojima, K., Fujita, Y., Nozawa, Y., Deguchi, T. & Ito, M. MiR-34a attenuates paclitaxel-resistance of hormone-refractory prostate cancer PC3 cells through direct and indirect mechanisms. *The Prostate* **70**, 1501-1512 (2010).
104. Chang, T.C. et al. Transactivation of miR-34a by p53 broadly influences gene expression and promotes apoptosis. *Molecular cell* **26**, 745-752 (2007).
105. Li, J. et al. Transcriptional activation of microRNA-34a by NF-kappa B in human esophageal cancer cells. *BMC molecular biology* **13**, 4 (2012).
106. Tweddle, D.A., Malcolm, A.J., Bown, N., Pearson, A.D. & Lunec, J. Evidence for the development of p53 mutations after cytotoxic therapy in a neuroblastoma cell line. *Cancer research* **61**, 8-13 (2001).
107. Schleiermacher, G. et al. Variety and complexity of chromosome 17 translocations in neuroblastoma. *Genes, chromosomes & cancer* **39**, 143-150 (2004).
108. Welch, C., Chen, Y. & Stallings, R.L. MicroRNA-34a functions as a potential tumor suppressor by inducing apoptosis in neuroblastoma cells. *Oncogene* **26**, 5017-5022 (2007).
109. White, P.S. et al. A region of consistent deletion in neuroblastoma maps within human chromosome 1p36.2-36.3. *Proceedings of the National Academy of Sciences of the United States of America* **92**, 5520-5524 (1995).
110. Schwarz, D.S. et al. Asymmetry in the assembly of the RNAi enzyme complex. *Cell* **115**, 199-208 (2003).

111. Rimokh, R. et al. Rearrangement of CCND1 (BCL1/PRAD1) 3' untranslated region in mantle-cell lymphomas and t(11q13)-associated leukemias. *Blood* **83**, 3689-3696 (1994).
112. Easton, J., Wei, T., Lahti, J.M. & Kidd, V.J. Disruption of the cyclin D/cyclin-dependent kinase/INK4/retinoblastoma protein regulatory pathway in human neuroblastoma. *Cancer research* **58**, 2624-2632 (1998).
113. Strieder, V. & Lutz, W. E2F proteins regulate MYCN expression in neuroblastomas. *The Journal of biological chemistry* **278**, 2983-2989 (2003).
114. Goldschneider, D. et al. Expression of C-terminal deleted p53 isoforms in neuroblastoma. *Nucleic acids research* **34**, 5603-5612 (2006).
115. Nabors, L.B., Gillespie, G.Y., Harkins, L. & King, P.H. HuR, a RNA stability factor, is expressed in malignant brain tumors and binds to adenine- and uridine-rich elements within the 3' untranslated regions of cytokine and angiogenic factor mRNAs. *Cancer research* **61**, 2154-2161 (2001).
116. Kim, H.H. et al. HuR recruits let-7/RISC to repress c-Myc expression. *Genes & development* **23**, 1743-1748 (2009).
117. Qi, L. et al. Expression of miR-21 and its targets (PTEN, PDCD4, TM1) in flat epithelial atypia of the breast in relation to ductal carcinoma in situ and invasive carcinoma. *BMC cancer* **9**, 163 (2009).
118. Wickramasinghe, N.S. et al. Estradiol downregulates miR-21 expression and increases miR-21 target gene expression in MCF-7 breast cancer cells. *Nucleic acids research* **37**, 2584-2595 (2009).
119. Chen, Y., Tsai, Y.H., Fang, Y. & Tseng, S.H. Micro-RNA-21 regulates the sensitivity to cisplatin in human neuroblastoma cells. *Journal of pediatric surgery* **47**, 1797-1805 (2012).